# Investigator's Brochure

**for**

# 3'-deoxy-3'-[F-18] fluorothymidine: [F-18]FLT

**An Investigational Positron Emission Tomography (PET) Radiopharmaceutical for Injection Intended for use as an In Vivo Diagnostic for Imaging Active Cellular Proliferation of Malignant Tumors.**



**IND # put your IND# here**

**Put your Name and Address here**

**IB Edition Number: 11**

**IB Edition Date/Release Date: February 19, 2021**

# Table of Contents

# II. INTRODUCTION

3'-deoxy-3'-[F-18] fluorothymidine [F-18]FLT is a structural analog of the DNA constituent, thymidine, that enters proliferating cells and is phosphorylated by human thymidine kinase 1, which is regulated during the cell cycle. The 3' substitution prevents further incorporation into replicating DNA, and the now ionic [F-18]FLT-MP is trapped inside proliferating cells. [F-18] decays with positron emission.

**Positron Emission Tomography**

Positron emission tomography (PET) is a quantitative tomographic imaging technique which produces cross-sectional images that are composites of volume elements (voxels). In PET images, the signal intensity in each voxel is dependent upon the concentration of the radionuclide within the target tissue (e.g., organ, tumor) volume. To obtain PET imaging data, the patient is placed in a circumferential detector array.

Patients will undergo two separate components for a typical PET imaging procedure. One component is a transmission scan via a CT scan. In the past a germanium rod source was used over the field-of-view of interest (specifically the tumor or the majority of the body with whole body PET/PET-CT imaging). This CT scan also provides limited anatomic information. The second component of the study is the emission scan which can be a dynamic imaging acquisition over a specific area of interest or multiple acquisitions over the whole body. The typical PET study takes about 20 minutes to 2 hours to perform depending on the nature of the acquisitions and the areas of the body that are imaged.

The patient can be prepared by fasting for 4 – 6 hours, although this is not required. After the [F-18]FLT tracer (approximately 5 mCi) is injected, imaging can commence immediately for a fully quantitative study over one area of the body, or imaging can be performed after an uptake period of about 60 – 90 minutes if whole body semi-quantitative imaging is being performed.

Although [F-18]FLT studies are designed to characterize FLT as a tracer of cellular proliferation in the primary tumor, comparison of [F-18]FLT images with other clinical imaging, and with surgical staging, will also provide data about [F-18]FLT's ability to depict regional tumor proliferation and distal metastases.

# III. [F-18]FLT PRODUCT AGENT DESCRIPTION

## 1. AGENT DESCRIPTION

3'-deoxy-3'-[F-18]fluorothymidine: [F-18]FLT (MW 243) is a structural analog of the DNA constituent, thymidine (Figure 1). It is a radiolabeled imaging agent that is produced by various

but equivalent syntheses that has been proposed for investigating cellular proliferation with positron emission tomography (PET). Since FLT is not incorporated into DNA, due to phosphorylation by thymidine kinase, (a part of the proliferation pathway) FLT-monophosphate (FLT-MP) is trapped in the cell. As such, it has the potential to facilitate imaging of proliferating tumor in proportion to the DNA synthesis rate. Clinical and nonclinical studies support the use of FLT as an imaging probe for quantifying cellular proliferation with positron emission tomography (PET). Therefore, FLT is proposed as a radiolabeled imaging probe for quantifying cellular proliferation in malignant tumors with PET.

## 2. CHEMICAL STRUCTURE

[F-18]FLT has not been marketed in the United States and, to the best of our knowledge; there has been no marketing experience with this drug in other countries. The radiopharmaceutical product, [F-18]FLT is the only active ingredient and it is dissolved in a solution of ≤ 10 mL of 0.01 M phosphate buffered saline (PBS): < 10% ethanol (v:v). The drug solution is stored at room temperature with an expiration time of 8 hours. The injectable dose of [F-18]FLT for most studies will be approximately 175 MBq (5 mCi) at the time of injection. In the dose of [F-18]FLT only a small fraction of the FLT molecules are radioactive. The amount of injected drug is ≤ 0.61 µg/mL (≤ 2.5 nmol/mL) of FLT. [F-18]FLT is administered to subjects by intravenous injection of ≤ 10 mL.

There is no evidence that nonradioactive and radioactive FLT molecules display different biochemical behavior.

**Figure 1. Chemical Structures**

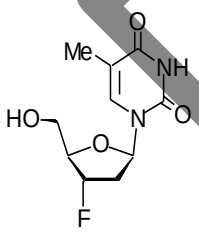


FLT

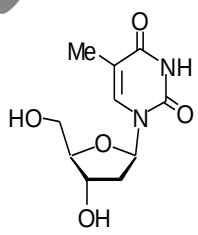


Thymidine

## 3. FINAL PRODUCT SPECIFICATIONS

The drug is composed of a small amount of [F-18]FLT that is labeled with radioactive F-18 at the 3'-position on the sugar ring with a specific activity above 200 Ci/mmol at the time of injection, as assured by the combined specifications of < 0.61 µg, ≤ 10 mL per dose and 5 mCi dose. The radiopharmaceutical product, [F-18]FLT is the only active ingredient and it is dissolved in a solution of ≤ 10 mL of 0.01 M phosphate buffered saline (PBS): < 10% ethanol (v:v). [F-18]FLT is administered to subjects by intravenous injection (≤ 10 mL).

**Table 1. Final Product Specifications**

| **SPECIFICATIONS** | |
|---|---|
| Radiochemical Purity (TLC): | $R_f$ = 0.4 – 0.7<br>Purity ≥ 95% |
| Residual Solvent Levels: | Acetone ≤ 5000 ppm<br>Acetonitrile ≤ 410 ppm<br>DMSO ≤ 5000 ppm |
| Radionuclidic Purity: | Measured half-life 100 – 120 minutes |
| Bacterial Endotoxin Levels: | < 175 EU per dose |
| pH: | 4.5-8.0 |
| Sterility: | no growth observed in 14 days, must pass filter test |
| Residual Kryptofix® [2.2.2]: | < 50 µg/ mL Kryptofix® |
| Radiochemical Purity (HPLC): | ≥95% |
| Chemical Purity (HPLC): | FLT ≤ 6.1 µg/dose |
| Chemical Purity (particulates): | Clear and Colorless |

The specifications for pH and acetonitrile have been updated. The purity specifications have been clarified to ≥ instead of > to avoid ambiguity. These changes are not considered major and will not increase risk to the patient and align these specifications with similar FDA approved PET radiopharmaceuticals. Many sites are now preparing FLT with pre-filled cassettes and automated synthesis instruments that were designed in compliance with these newer published limits.

1. Acetonitrile is listed in the Guidance for Industry, QC3 – Tables and List, Revision 2, February 2012 as a class 2 solvent with a concentration limit of 410 ppm. 2. FDA approved labeling for two very similar radiopharmaceuticals, F-18 FDG and NaF F18, has both drugs specified at pH 4.5-8. To be consistent with these drugs, we have changed the F-18 FLT specification to 4.5-8.

**Table 2. Final Product Components**

| COMPONENTS | | |
|---|---|---|
| [$^{18}$F]FLT, 3'-deoxy-3'-[$^{18}$F]fluorothymidine | same as for [F-19]FLT | ≤ 5.0 mCi |
| [$^{19}$F]FLT, 3'-deoxy-3'[$^{19}$F]fluorothymidine | NSC# 140025 for [F-19]FLT | ≤ 6.1 μg/dose |
| Sodium phosphates | USP | 0.01 M |
| Ethanol, absolute | USP | < 10% by volume |
| Saline for injection | USP | 0.15 M |

**Table 3. Final Product Impurities**

| IMPURITIES | | Highest Values in 2 Site Qualification Runs (n = 17) |
|---|---|---|
| Kryptofix [2.2.2.] | < 50 μg/ml | None detected |
| Acetonitrile | ≤ 410 ppm | 86 ppm |
| DMSO | ≤ 5000 ppm | 353 ppm |
| Acetone | ≤ 5000 ppm | 190 ppm |

# IV. PHARMACOLOGY

The pharmacology of FLT is based on its action as an inhibitor of DNA synthesis (Langen, 1969; 1972; 1972; Matthes, 1988). Intracellular metabolism of FLT produces nucleotides that inhibit endogenous DNA polymerases because they lack a 3'-hydroxyl substituent. This results in premature chain termination of DNA synthesis (Matthes 1987, Sundseth 1996). These biochemical properties can account for FLT's prominent hematological and liver toxicity in treatment studies. The proposed PET tracer studies using approximately 6 μg single dose [F-18]FLT are significantly lower than the oral 0.125 mg/kg or 2 mg/day multi dose used in the human studies (Flexner, 1994; Faraj, 1994; Sundseth, 1996; Katlama, 2004; Ghosn, 2007). The pharmacology of FLT closely parallels that of the widely used prescription HIV-antiviral drug azidothymidine (AZT) (Lundgren, 1991; Kong, 1992). Both FLT and AZT are 3'-deoxythymidine analogs that act as inhibitors of DNA synthesis and are cleared from the body in the same way. Although FLT is significantly more cytotoxic than AZT in test cell lines (Faraj, 1994) at comparable levels of exposure, this is not a factor when [F-18]FLT exposure is limited to typical PET imaging microdose requirements. Cellular uptake of FLT and thymidine is greater than that of AZT. Transport of FLT and thymidine across cell membranes occurs by active transport and passive diffusion (Kong, 1992).

# V. TOXICOLOGY AND SAFETY

## 1. MECHANISM OF ACTION FOR TOXICITY

Intracellular metabolism of FLT produces nucleotide phosphates that inhibit endogenous DNA polymerases and can prematurely chain terminate DNA (Matthes, 1987; Sundseth, 1996). These

biochemical properties can account for FLT's prominent hematological and liver toxicity when dose at high dose in treatment studies. The proposed PET tracer studies using approximately 6 µg single dose [F-18]FLT are a thousand fold lower than the oral 0.125 mg/kg multi-dose used in the human studies (Flexner, 1994; Faraj, 1994; Sundseth, 1996; Katlama, 2004; Ghosn, 2007).

## 2. [F-19] FLT ANIMAL TOXICITY STUDIES

A preliminary study of FLT's toxic effects was reported for cynomologus monkeys receiving multiple doses of FLT by subcutaneous (s.c.) injection (3 x 0.25 mg/kg s.c.; Lundgren, 1991). Table 4 lists the standard hematological parameters, liver enzymes, and serum creatinine for the FLT-treated monkeys and controls that were studied.

**Table 4. Laboratory Values for Cynomologus Monkey Study**

| | DAY 1 | DAY 0 | DAY 10 | | DAY 41 | |
|---|---|---|---|---|---|---|
| **Analyte** | **FLT** | **CONTROL** | **FLT** | **CONTROL** | **FLT** | **CONTROL** |
| Albumin (g/L) | 32 | 32 | 32 | 32 | 40 | 32 |
| Creatinine (µmol/L) | 83 | 88 | 68 | 75 | 76 | 75 |
| GGT (µkat/L) | 1.03 | 1.60 | 0.62 | 1.26 | 0.82 | 1.58 |
| SGOT (µkat/L) | 0.60 | 1.53 | 0.95 | 1.36 | 0.68 | 0.72 |
| SGPT (µkat/L) | 2.11 | 2.67 | 1.61 | 2.11 | 1.05 | 1.45 |
| CK (µkat/L) | 6.78 | 4.17 | 5.70 | 2.64 | 8.02 | 5.53 |
| LDH (µkat/L) | 33 | 36 | 29.2 | 35.2 | 28.5 | 25.2 |
| WBC ($x10^{-9}$/L) | 4.92 | 8.2 | 4.72 | 7.5 | 5.84 | 9.52 |
| RBC ($x10^{-12}$/L) | 6.06 | 5.6 | 4.9 | 4.71 | 5.74 | 5.78 |
| HGB (g/L) | 112 | 102 | 89 | 85 | 105 | 103 |
| HCT | 0.37 | 0.35 | 0.30 | 0.29 | 0.36 | 0.36 |
| PLT ($x10^{-9}$/L) | 332 | 414 | 246 | 348 | 352 | 430 |
| MCV (fl) | 61.6 | 62.9 | 59.8 | 62.0 | 62.0 | 62.1 |

Standard hematological parameters, liver enzymes and serum creatinine values for FLT treated (3 x 0.25 mg/kg; s.c.: n = 2) and controls (n = 4) for cynomologus monkeys (1.0 kat/l = 58.8U/L)

Unpublished studies filed to the NCI IND (studies are the property of Medivir) in mice, rats, and dogs reported only minor hematological effects at doses up to 900 mg/kg intravenously administered (iv) in mice and rats and 1000 mg/kg iv in dogs.

## 3. [F-18]FLT ANIMAL TOXICITY STUDIES

There are currently no published animal toxicity data for [F-18]FLT. Since the half-life of Fluorine 18 is only 109 minutes toxicity studies are not possible with the radiolabeled agent. The [F-19] data presented would be the basis for both animal and human toxicity characterization.

## 4. [F-19]FLT HUMAN TOXICITY

The pharmacology of FLT is based on its action as an inhibitor of DNA synthesis (Langen, 1969; 1972; 1972; Matthes, 1988). This is the mechanism of the toxicity that is seen with the drug. Intracellular metabolism of FLT produces FLT-phosphates but these nucleotides inhibit endogenous DNA polymerases because they lack a 3'-hydroxyl substituent. This results in premature chain termination of DNA synthesis (Matthes 1987, Sundseth 1996). These biochemical properties can account for FLT's prominent hematological and liver toxicity (Flexner, 1994; Faraj, 1994; Sundseth, 1996). The pharmacology of FLT closely parallels that of the widely used prescription HIV-antiviral drug azidothymidine (AZT) (Lundgren, 1991; Kong, 1992). Both FLT and AZT are 3'-deoxythymidine analogs that act as inhibitors of DNA synthesis and are cleared from the body in the same way. However, FLT is significantly more cytotoxic than AZT in test cell lines (Faraj, 1994). Cellular uptake of FLT and thymidine is greater than that of AZT. Transport of FLT and thymidine across cell membranes occurs by active transport and passive diffusion (Kong, 1992).

FLT was investigated as an oral anti-AIDS drug in humans (Flexner 1994). Toxic effects and death were reported for some subjects receiving FLT during randomized concentration-controlled trials during a 16-week treatment of oral multi-dosing. Doses of 0.125 mg/kg every 12 hours, produced a mean cumulated drug exposure ($AUC_{12}$: area under curve) of 417 ng-h/mL. At this level, serious (grade 3) hematologic toxicity occurred in 6 of 10 subjects. At 300 ng-h/mL, grade 2 or greater (fall in hemoglobin to ≤ 9.4 g/dL) anemia developed within four weeks in 9 of 12 subjects. At 200 ng-h/mL almost no clinically significant anemia developed, but dose-limiting granulocytopenia (< 750 granulocytes/$mm^3$) occurred in 5 of 14 subjects. Mild peripheral neuropathy occurred in 2 of 15 subjects at 50 ng-h/mL, but was not dose-limiting.

FLT drug trials were terminated after two subjects died unexpectedly of hepatic failure. One of these subjects, who was assigned to 200 ng-h/mL, developed progressive liver failure and died after 12 weeks of FLT therapy. A second subject, receiving a fixed dose of 10 mg/day, developed progressive liver failure and died at 12 weeks. All surviving subjects were followed closely for four weeks after stopping FLT and none had evidence of clinically significant liver disease or other adverse effects. Overall, 25 of the 44 subjects receiving at least two doses of FLT completed the 16-week study without clinically significant adverse effects.

FLT (Alovudine) was withdrawn from development for several years, and then reinvestigated for multi-drug resistant HIV infection. Fifteen patients with multi-drug resistance HIV received

7.5 mg each day for 28 days along with their on-going therapy (Katlama, 2004). No serious adverse events were observed.

A randomized, double-blind, placebo-controlled trial investigating three doses of alovudine (0.5, 1 and 2 mg) or placebo added for four weeks to a failing regimen in patients with evidence of NRTI resistant HIV strains. Seventy-two patients were enrolled in the study: 21, 13, 18, and 20 in the placebo and 0.5, 1, and 2 mg arms, respectively. There was no significant change in CD4 cell count. Alovudine was well tolerated; diarrhea and nausea were reported in up to one-third of the patients and mean hemoglobin decreased slightly in the highest dose group (Ghosn, 2007).

## 5. [F-18]FLT HUMAN TOXICITY STUDIES

Since the half-life of fluorine 18 is only 109 minutes toxicity studies are not possible with the radiolabeled agent. The [F-19] data presented would be the basis for both animal and human toxicity characterization.

It is important to note that [F-19] clinical repeat dosing, as reported above, results in total exposure that is up to several thousand times greater, as measured by $AUC_{12}$, than that produced by typical [F-18] dosing in a PET imaging setting.

## 6. [F-18]FLT HUMAN SAFETY STUDIES

In a study performed at the University of Washington, Turcotte and colleagues (Turcotte, 2008) assessed the toxicity of [F-18]FLT in twenty patients with proven or suspected diagnosis of non-small cell lung cancer (Table 5). Blood samples were collected for each patient at multiple times before and after [F-18]FLT-PET and assayed for comprehensive metabolic panel, total bilirubin, complete blood and platelet counts. In addition, a standard neurological examination by a qualified physician was performed for each patient before and immediately after [F-18]FLT-PET. All [F-18]FLT doses were calculated based on patient weight (2.59 MBq/kg = 0.07 mCi/kg) with a maximal dose of 185 MBq (5.0 mCi). Starting with the [F-18]FLT injection, dynamic PET images were acquired for 90 or 120 minutes. By placing a region-of-interest in the center of the left ventricular chamber, blood time-activity curves were generated for each patient from the dynamic PET data and then extrapolated to 720 minutes. This provided a measure of the area under the [F-18]FLT concentration curve for 12 hours ($AUC_{12}$). A separate estimation of the $AUC_{12}$ was also obtained from sequential blood samples collected during PET data acquisition. No side effects were reported by patients or observed. No change was observed in the neurological status of patients. A neurological examination was performed by an experienced neurologist prior to [F-18]FLT administration, the day after [F-18]FLT administration, and at four weeks post [F-18]FLT administration. Only albumin, red blood cell count, hemoglobin, and hematocrit show a statistically significant decrease over time (Table 5). These changes were attributed to IV hydration during PET imaging and to subsequent blood loss at surgery. The $AUC_{12}$ values estimated from imaging data are not significantly different from those found from

serial measures of [F-18]FLT blood concentrations (P = 0.66). No significant neurologic sequelae have been attributed to [F-18]FLT use in pet imaging to date. As a result, peripheral neuropathy, which had been listed as a possible risk based upon observations at significantly higher doses in early therapeutic HIV studies, is no longer considered a risk of [F-18]FLT use in a micro-dose imaging setting. Screening for peripheral neuropathy is not justified based upon the available evidence in multiple [F-18]FLT imaging trials.

**Table 5. Laboratory Values (mean ± SD) At Each Time Point**

| | Pre-[F-18]FLT | Immediate < 5 hours | 5 – 24 hours | 1 – 7 days | > 1 week | P* |
|---|---|---|---|---|---|---|
| Sodium (mEq/L ± SD) | 139.4 ± 1.5 | 138.2 ± 2.1 | 138.3 ± 2.0 | 137.5 ± 1.8 | 138.1 ± 2.3 | 0.064 |
| Potassium (mEq/L ±S D) | 4.2 ± 0.5 | 4.2 ± 0.4 | 4.1 ± 0.4 | 4.2 ± 0.3 | 4.2 ± 0.4 | 0.968 |
| Chloride (mEq/L ± SD) | 102.3 ± 3.3 | 104.2 ± 3.7 | 104 ± 3.8 | 102.3 ± 2.4 | 101.2 ± 3.1 | 0.055 |
| Glucose (mEq/L ± SD) | 95.1 ± 14.8 | 96.6 ± 20.7 | 98.5 ± 23.1 | 105.4 ± 17.7 | 109.5 ± 14.6 | 0.175 |
| Creatinine (mEq/L ± SD) | 0.885 ± 0.198 | 0.882 ± 0.207 | 0.881 ± 0.180 | 0.910 ± 0.190 | 0.844 ± 0.217 | 0.949 |
| BUN (mEq/L ± SD) | 15.8 ± 5.0 | 15.1 ± 5.6 | 15.2 ± 6.3 | 14.3 ± 5.2 | 15.3 ± 5.7 | 0.959 |
| SGOT (U/L ± SD) | 20.8 ± 5.0 | 22.0 ± 5.1 | 22.0 ± 5.3 | 22.2 ± 11.4 | 21.8 ± 6.7 | 0.973 |
| SGPT (U/L ± SD) | 18.7 ± 6.7 | 18.5 ± 6.6 | 19.1 ± 6.5 | 17.6 ± 5.3 | 17.2 ± 6.5 | 0.978 |
| Albumin (g/dL ± SD) | 3.9 ± 0.5 | 3.5 ± 0.4 | 3.44 ± 0.3 | 3.1 ± 0.6 | 3.2 ± 0.8 | 0.003 |
| Alk Phos (U/L ± SD) | 73.8 ± 19.4 | 61.1 ± 14.7 | 58.3 ± 17.0 | 59.5 ± 22.7 | | 0.081 |
| Bilirubin (mg/dL ± SD) | 0.647 ± 1.81 | 0.573 ± 0.246 | 0.581 ± 0.263 | 0.621 ± 0.286 | 0.752 ± 0.418 | 0.714 |
| RBC ($X10^9$ /ml ± SD) | 4.5 ± 0.4 | 4.3 ± 0.5 | 4.2 ± 0.5 | 3.8 ± 0.3 | 3.7 ± 0.4 | <0.0001 |
| Hematocrit (% ± SD) | 40.9 ± 3.1 | 39.1 ± 4.4 | 38.4 ± 4.0 | 35.2 ± 3.4 | 35.0 ± 3.4 | <0.0001 |
| WBC ($X10^6$/ml ±S D) | 7.6 ± 2.1 | 7.7 ± 3.4 | 7.9 ± 3.3 | 9.5 ± 2.8 | 9.0 ± 3.2 | 0.262 |
| Platelets ($X10^6$/ml ± SD) | 278.1 ± 96.9 | 259.1 ± 103.1 | 255.9 ± 103.0 | 230.1 ± 76.7 | 233.5 ± 69.5 | 0.674 |

*one-way ANOVA P values (from Turcotte et al, 2007)

The single dose $AUC_{12}$ values derived from blood clearance studies performed at the University of Washington ranged from 0.22 to 1.34 ng-h/mL with a mean of 0.80 ng-h/mL. This range corresponds to 0.46% to 2.7% of the Flexner therapeutic clinical trial $AUC_{12}$ of 50 ng-h/mL. In the Flexner trial the only dose-limiting toxicity was hematologic, either anemia or granulocytopenia, and the threshold for this response was greater than 50 ng-h/mL. The only adverse event at the 50 ng-h/mL level was a peripheral neuropathy in 2 of 15 patients that manifested at about 40 days. The peripheral neuropathy was detected by vibration sensation scores and was not a dose limiting toxicity. For FLT, the average arterial blood curve (% injected dose per mL of blood) from 16 University of Washington FLT two-hour studies were extrapolated to 12 hours using the conservative estimation that there would be no more clearance of FLT from the plasma and that all the radioactivity in the blood was in the form of the unmetabolized FLT. It was then assumed that 100% of the dose (6.1 µg = 6100 ng) was in a plasma volume of 3,000 mL. The dose in nanograms was multiplied by the fraction of the injected dose per mL divided by the plasma volume to obtain ng/mL for each time point. The area under this curve was 0.5 ng-h/mL. Thus, the $AUC_{12}$ of a single injected dose of FLT will be < 1% of the single dose and less than 0.01% of the cumulative 40- day dose of the lowest mass

associated with any reported toxic effect in humans, 50 ng-h/mL and will not lead to clinically detectable toxic effects.

An NCI-sponsored study (Spence, 2008) was conducted at University of Washington in Seattle beginning in 2005. Twelve patients with brain tumors were enrolled. Overall, 2 of the 12 subjects receiving FLT experienced an elevation in BP from baseline to two hours post infusion: Subjects 1 (119/56 – 133/66) and 4 (120/78 – 163/74). In Subject 4, abnormal BP was attributed to discomfort from the head immobilization device. There were no clinically relevant events reported. All subjects performed consistently on the pre- and post- neurological exams and there were no changes in status. The clinical chemistry data are shown in Table 6.

Four of these analytes demonstrated statistically significant changes on one-way ANOVA: potassium, carbon dioxide, total protein, and albumin. Some of the other values were above or below normal, but no pattern was seen except that many were lower on the day of the study. These decreases are attributed to two main factors. Normal saline infusion, which expands blood volume, and arterial blood sampling for kinetic analysis are performed during the procedure, both of which will cause a general lowering of the concentration of blood components. The subsequent recovery of these values to baseline is consistent with this explanation and consistent with the results obtained by Turcotte (2008).

The $AUC_{12}$ values, estimated from assaying arterial blood samples, ranged from 0.004 to 0.035 ng-hr/ml, with a mean of 0.016 ng-hr/ml. These mass levels correspond to 0.008% to 0.07% of the least toxic single dose of 50 ng-hr/ml in the Flexner trial (a 40-day, 2 dose per day study). If comparison is made to the cumulative dose, the [F-18]FLT is at 0.0001% to 0.0009% of the therapeutic dose.

**Table 6. Laboratory Values (mean ± SD) At Each Time Point**

| Analyte | Pre Mean ± SD | Immediately Pre-Mean ± SD | Day 1 Mean ± SD | Day 28 Mean ± SD |
|---|---|---|---|---|
| Amylase | 75.4 ± 23.1 | 68.5 ± 27.6 | 77.8 ± 33.9 | 75.4 ± 33.7 |
| Na+ | 140.8 ± 2.6 | 138.4 ± 4.6 | 139.3 ± 3.3 | 141.1 ± 3.1 |
| K+ | 4.27 ± 0.42 | **3.88* ± 0.20** | 4.20 ± 0.28 | 4.08 ± 0.30 |
| Cl- | 106.0 ± 3.7 | 106.0 ± 4.6 | 104.5 ± 3.6 | 106.5 ± 3.3 |
| CO2 total | 27.6 ± 2.9 | **24.6* ± 2.3** | 26.9 ± 2.1 | 26.8 ± 2.5 |
| Ion Gap | 6.29 ± 1.60 | 7.83 ± 2.29 | 7.70 ± 2.21 | 7.67 ± 3.08 |
| Glucose | 121.8 ± 47.7 | 98.7 ± 33.4 | 125.2 ± 73.5 | 116.9 ± 71.6 |
| BUN | 12.45 ± 4.06 | 10.58 ± 4.01 | 11.00 ± 3.03 | 13.73 ± 4.63 |
| Creatinine | 1.00 ± 0.17 | 0.85 ± 0.17 | 0.97 ± 0.24 | 1.01 ± 0.27 |
| Protein total | 6.45 ± 0.38 | **5.66* ± 0.37** | 6.14 ± 0.57 | 6.33 ± 0.76 |
| Albumin | 4.15 ± 0.25 | **3.66* ± 0.18** | 4.01 ± 0.51 | 3.99 ± 0.50 |
| Bilirubin total | 0.68 ± 0.16 | 0.79 ± 0.24 | 0.79 ± 0.17 | 0.65 ± 0.12 |
| Ca++ | 9.35 ± 0.19 | 9.01 ± 0.29 | 9.38 ± 0.39 | 9.24 ± 0.54 |
| AST (GOT) | 26.3 ± 5.9 | 22.5 ± 4.4 | 23.7 ± 5.0 | 26.8 ± 5.1 |
| Alk Phos | 86.0 ± 22.7 | 78.5 ± 26.4 | 84.3 ± 27.9 | 86.5 ± 30.3 |
| GPT | 39.4 ± 15.8 | 30.2 ± 9.6 | 32.7 ± 11.2 | 33.0 ± 7.7 |
| GGT | 44.7 ± 21.1 | 42.3 ± 22.4 | 47.2 ± 23.3 | 44.3 ± 26.0 |
| LDH | 224.9 ± 104.9 | 151.8 ± 41.9 | 174.9 ± 57.9 | 248.6 ± 205.4 |
| Phosphate | 3.15 ± 0.55 | 3.03 ± 0.55 | 3.16 ± 0.59 | 3.07 ± 0.41 |
| Prothrombin | 12.74 ± 1.39 | 13.59 ± 0.52 | 13.12 ± 0.94 | 12.82 ± 1.39 |
| INR | 1.02 ± 0.04 | 1.05 ± 0.05 | 1.01 ± 0.09 | 1.01 ± 0.06 |
| PTT | 26.8 ± 3.1 | 29.4 ± 5.7 | 30.9 ± 15.8 | 26.3 ± 2.8 |
| WBC | 6.13 ± 1.91 | 5.75 ± 1.40 | 6.96 ± 3.98 | 5.85 ± 2.10 |
| RBC | 4.65 ± 0.42 | 4.37 ± 0.39 | 4.50 ± 0.38 | 4.48 ± 0.52 |
| Hgb | 14.5 ± 1.1 | 13.4 ± 0.9 | 13.9 ± 1.1 | 13.9 ± 1.6 |
| Hct | 42.5 ± 3.1 | 39.9 ± 3.4 | 41.1 ± 3.0 | 41.2 ± 4.5 |
| MCV | 91.5 ± 3.3 | 91.3 ± 3.5 | 91.3 ± 3.2 | 92.1 ± 3.3 |
| MCH | 31.4 ± 1.6 | 30.8 ± 1.4 | 31.0 ± 1.4 | 31.2 ± 1.3 |
| MCHC | 34.3 ± 0.9 | 33.7 ± 0.8 | 33.9 ± 0.6 | 33.9 ± 0.8 |
| Platelets | 233.9 ± 54.2 | 226.2 ± 42.7 | 220.9 ± 47.8 | 220.0 ± 52.4 |
| ANC | 4.08 ± 1.42 | 3.79 ± 1.15 | 5.02 ± 3.34 | 3.89 ± 1.42 |
| Spec Gravity | 1.02 ± 0.01 | 1.01 ± 0.00 | 1.02 ± 0.00 | 1.02 ± 0.00 |
| pH | 6.05 ± 1.01 | 6.88 ± 0.80 | 6.60 ± 0.97 | 5.85 ± 1.08 |

* statistically significant change ($p < 0.05$); one-way ANOVA

The published studies on [F-18]FLT are discussed in Section VII of this Investigator's Brochure. While none of these studies reported explicit safety information, the majority of these publications did indicate that Institutional Review Board (IRB) or Ethics Committee approval was obtained for the study, so the patients would have been observed for clinically evident adverse events, none of which were reported.

## 7. [F-19] GENOTOXICITY AND MUTAGENICITY

There are some literature reports on the mutagenic properties of FLT. Ehrlich ascites tumor cells incubated with 10 µM FLT for extended periods (12, 24, 36 hours: AUC 120, 240, 360 nmol-h/mL) showed chromosome damage (Wobus, 1976). The most prominent effects were breaks and gaps, however, much less damage was seen if a recovery time was included (12, 24 h) and the damage could also be largely reversed by post-treatment with thymidine (10 µM). FLT anabolism, FLT incorporation into DNA and the effects of FLT on cellular genome integrity have been studied in cultured CEM ($CD4^+$ human lymphoblastoid) cells (Sundseth, 1996). FLT concentrations of 10 and 100 µM produced chromosome fragmentation characteristic of cells undergoing apoptosis. In contrast, at 1 µM FLT the level of fragmentation was similar to the controls without FLT exposure. Despite prominent levels of intracellular FLT anabolites, the fraction of FLT in DNA was low ($10^{-6}$ total). At the minimum specific activity permitted by the overall specifications, the dose to patients (5 mCi) will correspond to an initial, maximal plasma concentration of about 5 nM. This is 200 times lower than the level of FLT where no chromosomal damage was seen in CEM cells (1 µM). Based on these data, the administration of approximately 5 mCi of FLT to humans does not pose a probable threat of mutagenesis.

## 8. ADVERSE EVENTS AND MONITORING FOR TOXICITY

As discussed above, the mechanism of action of FLT's toxicity at therapeutic dosing levels is based on inhibition of DNA synthesis (Langen, 1969; 1972; 1972; Matthes, 1988). Total exposure to the radiolabeled agent for PET imaging, will be several thousand times lower than the exposure at which toxicity has been observed in humans. Nevertheless, as with all investigational drugs, patients receiving FLT should be observed for adverse events, and promptly treated should any adverse effects occur.

In the Flexner HIV therapeutic dosing study mild peripheral neuropathy occurred in 2 of 15 subjects at 50 ng-h/mL, but was not dose-limiting. In the Katlama study, no serious adverse events were observed. Four patients experienced fatigue, three experienced loss of appetite, two grade 1 and one grade 2 transaminase elevations and one fall in hemoglobin. In a recent randomized, double-blind placebo-controlled study of NRTI-resistant HIV patients a four-week course of 2 mg/day FLT significantly reduced their viral load and showed no significant signs of toxicity (Ghosn, 2007).

In considering potential adverse effects that may be reasonably anticipated, based upon the available evidence for [F-18]FLT use in imaging, it is critical to note that for a single imaging study, at the minimum specific activity permitted by the overall specifications, the dose to patients receiving ≤ 5.0

mCi will correspond to an FLT injected mass of 25 nmoles. This is 10,000 times less than the cumulative dose of 56 mg, and 300 times lower than the daily 2 mg dose of FLT used in the most recent therapeutic patient studies.

Based on these data, the administration of a total 10 – 15 mCi of [F-18]FLT over several imaging time points required to assess the effects of therapeutic intervention (baseline and typically two time points during therapy) to humans poses a minimal risk for an adverse effect. Therefore, the risk profile for [F-18]FLT used as described in this Investigator's Brochure consists of allergic reaction/anaphylaxis, which appears to be highly unlikely, and risks that would be associated with any clinical IV infusion/injection.

# VI. BIODISTRIBUTION AND RADIATION DOSIMETRY OF [F-18]FLT

## 1. MOUSE BIODISTRIBUTION

Preclinical development of [F-18]FLT was undertaken at the University of Washington; studying the uptake of FLT in cultured tumor cells, biodistribution studies with rodents (Rasey, 2002) and monkeys and PET imaging in monkeys. Tumor cell cultures with a high S-phase fraction strongly sequester and retain labeled FLT and this uptake is proportional to the percentage of cells in S-phase. On this basis, imaging tumors with [F-18]FLT and modeling of data is designed to visualize regions of proliferation (high S-phase fraction).

## 2. NON-HUMAN PRIMATE BIODISTRIBUTION

Investigators at the University of Washington imaged four juvenile male monkeys (*Macaca nemestrina*): two normal monkeys and two acutely infected with human HIV. Approximately 4 mCi of [F-18]FLT was injected intravenously over 60 seconds and images were taken for 120 minutes. Blood samples were withdrawn via an arterial line, initially at 10 second intervals and then at progressively longer times. This study provided estimates of organ specific dosimetry in a species closely related to humans.

Table 7 shows the biodistribution data. The data showed the following primary observations: (i) [F-18]FLT was avidly taken up in normally proliferating tissue, such as bone marrow; (ii) blood [F-18]FLT levels fell to low background levels within 20 minutes, (iii) [F-18]FLT and its primary metabolite cleared by the kidneys into urine (30-50% of the injected dose within two hours); (iv) the two HIV infected animals that were autopsied after imaging showed elevated levels of radioactivity (twice marrow levels) in lymphoid tissues, such as spleen and lymph nodes. These data are consistent with the more complete human data shown in the next section.

**Table 7. [F-18]FLT Biodistribution in Juvenile Male *Macaca Nemestrina* Infected with Human HIV**

| SAMPLE/TISSUE | UPTAKE : Ci/g |
|---|---|
| Urine | 18.00 |
| Spleen | 4.22* ; 3.86* |
| Ileum | 2.04 |
| Bone marrow | 2.01 ; 1.78 |
| Colon | 1.67 ; 1.66 |
| Jejunum | 1.49 |
| Duodenum | 1.41 |
| Liver | 0.81 ; 0.65 |
| Testes | 0.27 ; 0.27 |
| Muscle (right, left leg) | 0.15 ; 0.13 |
| Pectoralis | 0.14 ; 0.13 |
| Cerebellum | 0.09 |
| Brainstem | 0.09 |
| Cortex | 0.08 ; 0.08 |

## 3. HUMAN RADIATION DOSIMETRY OF [F-18]FLT

The table noted below is from Table C.39 of the 2015 ICRP 128 publication. For additional information, please see the 2003 Vesselle article which contains dosimetry information from 18 cancer patients and the 2018 Mendes phantom model study, which includes dose recalculations for both ICRP 128 and the Vesselle data.

**Table 8. Radiation Dose to Patients from Radiopharmaceuticals**

**Obsorbed Doses of 3'-deoxy-3'-[F-18] fluorothymidine: Obsorbed Dose Per Unit Activity Administered (mGY MBq$^{-1}$)**

| Organ | Adult | 15 years | 10 years | 5 years | I year |
|---|---|---|---|---|---|
| Adrenals | 1.6E-02 | 1.9E-02 | 2.9E | 4.4E_02 | 7.7E-02 |
| Bone surfaces | 1.9E-02 | 2.4E-02 | 3.7E—02 | 6. IE-02 | 1.3E-01 |
| Brain | 8.2E-03 | 1.0E—02 | 1.7E—02 | 2.8E—02 | 5.2E-02 |
| Breast | 8.2E-03 | 1.OE-02 | 1.6E—02 | 2.5E-02 | 4.9E-02 |
| Gallbladder wall | 1.8E-02 | 2.1E-02 | 3.0E-02 | 4.6E-02 | 8.5E-02 |
| Gastrointestinal tract Stomach wall | 1.2E-02 | 1.4E-02 | 2.2E02 | 3.5E-02 | 6.6E-02 |
| Small intestine wall | 1.3E-02 | 1.6E-02 | 2.5E-02 | 3.8E-02 | 6.9E-02 |
| Colon wall | 1.2E-02 | 1.5E-02 | 2.3E-02 | 3.6E-02 | 6.5E-02 |
| Upper large intestine wall | 1.3E-02 | 1.5E-02 | 2.4E-02 | 3.8E-02 | 6.9E-02 |
| Lower large intestine wall | 1.2E-02 | 1.4E-02 | 2.2E-02 | 3.4E-02 | 5.9E-02 |
| Heart Wall | 1.2E-02 | 1.5E-02 | 2.4E-02 | 3.6E02 | 6.5E-02 |
| Kidneys | 4.3E-02 | 5.1E-02 | 7.2E-02 | 1.1E-01 | 1.9E-01 |
| Liver | 4.8E-02 | 6.3E-02 | 9.4E-02 | 1.4E-01 | 2.6E-01 |
| Lungs | 1.1E-02 | 1.4E-02 | 2.1E-02 | 3.2E-02 | 6.0-E02 |
| Muscles | 9.8E-03 | 1.2E-02 | 1.9E-02 | 3.0E-02 | 5.6E-02 |
| Esophagus | 9.8E-03 | 1.3E-02 | 1.9E-02 | 3.0E-02 | 5.6E-02 |
| Ovaries | 1.2E-02 | 1.5E-02 | 2.4E-02 | 3.6E-02 | 6.6E-02 |
| Pancreas | 1.5E-02 | 1.9E-02 | 2.9E-02 | 4.4E-02 | 7.9E-02 |
| Red marrow | 2.6E-02 | 3.0E-02 | 4.8E-02 | 8.6E-02 | 1.9E-01 |
| Skin | 7.5E-03 | 9.2E-03 | 1.5E-02 | 2.4E-02 | 4.6E-02 |
| Spleen | 2.2E-02 | 3.1E-02 | 4.7E-02 | 7.3E-02 | 1.3E-01 |
| Testes | 8.8E-03 | 1.1E-02 | 1.7E-02 | 2.7E-02 | 5.2E-02 |
| Thymus | 9.8E-03 | 1.3E-02 | 1.9E-02 | 3.0E-02 | 5.6E-02 |
| Thyroid | 9.4E-03 | 1.2E-02 | 1.9E-02 | 3.1E-02 | 5.8E-02 |
| Urinary bladder wall | 2.3E-02 | 2.8E-02 | 4.2E-02 | 6.2E-02 | 9.2E-02 |
| Uterus | 1.2E-02 | 1.5E-02 | 2.4E-02 | 3.7E-02 | 6.6E-02 |
| Remaining organs | 1.0E-02 | 1.3E-02 | 2.0E-02 | 3.3E-02 | 6.0E-02 |
| Effective dose (mSv MBq-1 | 1.5E-02 | 1.9E-02 | 2.9E-02 | 4.6E-02 | 8.8E-02 |

*The physical half-life of $^{18}$F is 1.83 h.*

## VII. [F-18]FLT PREVIOUS HUMAN EXPERIENCE

Preliminary studies using [F-18]FLT for imaging human subjects have been published (Table 13). [F-18]FLT has been studied for imaging in Germany and in the United States (e.g., UCLA, University of Washington in Seattle, Wayne State University). Imaging protocols used in Germany and the U.S. were pre-approved by their respective regulating committees and done under the Radioactive Drug Research Committee (RDRC) process. Patients received from 1.4 – 11 mCi of [F-18]FLT.

Since these early studies many sites have published studies in a wide variety of organ systems and diseases. These and other studies are summarized in Table 9 below.

**Table 9. A Summary of Published Manuscripts Reporting [F-18]FLT Human Imaging Studies**

| Year | Organ system | N | mCi injected (mean) | MBq Injected (mean) | Reference |
|---|---|---|---|---|---|
| 2020 | Cervical Cancer | 39 | 9.8+2.03 | 364 ± 75 | Cegła (2020) |
| 2020 | Cervical Cancer | 50 | 0.13 | 5MBq | Chopra (2020) |
| 2017 | Blood | 10 | 0.08/kg | 2.96/kg | Han (2017) |
| 2019 | Prostate | 17 | 9.3 | 345 | Scarpelli (2019) |
| 2017 | Prostate | 7 | 4.96–9.72 | 184–360 | Kairemo (2017) |
| 2020 | Lung | 63 | 0.13<br>Max=9.4 | 5<br>Max=350 | Christensen (2020) |
| 2019 | Lung | 10 | 10 | 370 | Cysouw (2019) |
| 2019 | Lung | 50 | 5 | 185 | Umeda (2019) |
| 2018 | Lung | 17 | 10 | 370 | Iqbal (2018) |
| 2017 | Lung | 55 | 0.1/kg | 3.7/kg | Wang (2017) |
| 2017 | Lung | 9 | 10 | 370 | Crandall (2017) |
| 2017 | Lung | 60 | 0.1/kg | 3.7/kg | Everitt (2017) |
| 2015 | Lung | 9 | 4.1-10.3 | 151-381 | Hoyng (2015) |
| 2015 | Lung | 23 | | | Liu (2015) |
| 2015 | Lung | 12 | 8.1-10.8 | 300-400 | Chen (2015) |
| 2014 | Lung | 15 | 5.5 – 8.8 | 205-327 | Bhoil (2014) |
| 2014 | Lung | 10 | 10 | 370 | Frings (2014) |
| 2014 | Lung | 20 | 0.1/kg | 3.7/kg | Everitt (2014) |
| 2014 | Lung | 60 | 0.1/kg | 3.7/kg | Leimgruber (2014) |
| 2014 | Lung | 7 | 6.9-9.8 | 254–361 | Trigonis (2014) |
| 2013 | Lung | 62 | 0.12/kg | 4.5/kg | Beauregard (2013) |
| 2013 | Lung | 14 | 6.76 | 250 | Frings (2013) |
| 2013 | Lung | 14<br>9 | 6.76<br>9.50 | 250<br>350 | Frings (2013) |
| 2013 | Lung | 40 | 8.1 | 300 | Scheffler (2013) |

| Year | Organ system | N | mCi injected (mean) | MBq Injected (mean) | Reference |
|---|---|---|---|---|---|
| 2013 | Lung | 162 | 0.1/kg | 4~5/kg | Xu (2013) |
| 2012 | Lung | 30 | 8.4±91 | 311±91 | Kobe (2012) |
| 2012 | Lung | 30 | 8.2±89 | 305±89 | Kahraman (2012) |
| 2012 | Lung | 1 | - | - | Scheffler (2012) |
| 2012 | Lung | 68 | 8.1-10.8 | 300-400 | Yang (2012) |
| 2011 | Lung | 34 | 8.1 | 300 | Zander (2011) |
| 2011 | Lung | 20 | 8.1 | 300 | Saga (2011) |
| 2011 | Lung | 50 | 7 | 259 | Mileshkin (2011) |
| 2011 | Lung | 25 | 0.07/kg<br>Max=5 | 2.59/kg<br>Max=185 | Brockenbrough (2011) |
| 2010 | Lung | 73 | 8.1–10.8 | 300-400 | Xu (2010) |
| 2010 | Lung | 31 | 8.1–10.8 | 300–400 | Yang (2010) |
| 2010 | Lung | 21 | 8 mCi | 300 | Koizumi (2010) |
| 2008 | Lung | 9 | 7.9-10.5 | 292-389 (373) | Shields (2008) |
| 2008 | Lung | 28 | 15 | 555 | Sohn (2008) |
| 2008 | Lung | 54 | 2.7-6.4 | 101-238 (158) | Yamamoto (2008) |
| 2008 | Lung | 34* | 8.1-10.8 | 300-400 | Yamamoto (2008) |
| 2008 | Lung | 55 | 8.1-10.8 | 300-400 | Tian (2008) |
| 2007 | Lung | 20 | 0.07 /kg | 2.6 /kg | Turcotte (2007) |
| 2008 | Lung | 54 | Mean 3.51<br>2.73-6.43 | Mean 129.9<br>101-238 | Yamamoto (2008) |
| 2007 | Lung | 18* | 3.92 | 145±26 | Yamamoto (2007) |
| 2006 | Lung | 11 | 5.0 | 185 | Yap (2006) |
| 2005 | Lung | 47 | 7.2-10.0 | 265-370 | Buck (2005) |
| 2005 | Lung | 17 | Max 5<br>0.07/kg | Max 185<br>2.6 /kg | Muzi (2005) |
| 2004 | Lung | 17 | 5.7<br>3.5-11.4 | Mean=210<br>130-420 | Cobben (2004) |
| 2004 | Lung | 28 (a) | 9.0<br>7.2-10.0 | Mean=334<br>265-370 | Halter (2004) |

| Year | Organ system | N | mCi injected (mean) | MBq Injected (mean) | Reference |
|---|---|---|---|---|---|
| 2003 | Lung | 16 | 5.4-10.8 | 200-400 | Dittman (2003) |
| 2003 | Lung | 26* | 9.0<br>7.2-10.0 | Mean=334<br>265-370 | Buck (2003) |
| 2002 | Lung | 30 (c) | 9.0<br>7.2-10.0 | Mean=334<br>265-370 | Buck (2002) |
| 2002 | Lung | 10* | 5.0 | 185 max | Vesselle (2002) |
| 2008 | Lung/Head/Neck | 9/6 | 10 | 370 | De Langen (2008) |
| 2013 | Thyroid | 20 | 0.1/kg | 3.7/kg | Nakajo (2013) |
| 2012 | Thyroid | 1 | 0.1 | 3.7/kg | Nakajo (2012) |
| 2016 | Pelvis | 32 | 0.07/kg | 2.6/kg | McGuire (2016) |
| 2015 | Ovarian | 6 | 8.0-10.0 | 296-370 | Cho (2015) |
| 2011 | Ovarian | 6 | 5 | 185 | Richard (2011) |
| 2017 | Oropharynx | 20 | 0.2/kg | 7.4/kg | Qi (2017) |
| 2012 | Oropharynx | 13 | 0.1/kg | 5.2/kg | Nyflot (2012) |
| 2015 | Renal | 20 | 5 | 185 | Horn (2015) |
| 2015 | Adrenal | 43 | 0.1/kg | 3.7/kg | Nakajo (2015) |
| 2012 | Uterus | 15 | 8.6-11.5 | 319-424 | Yamane (2012) |
| 2012 | Stomach | 1 | 5 | 185 | McKinley (2012) |
| 2012 | Liver | 20 | 5.68 | 210 | Contractor (2012) |
| 2018 | Blood | 8 | 6.7<br>mean = 6.4 | 250<br>mean = 236 | Sachpekidis (2018) |
| 2010 | Blood | 8 | 5 | 185 | Vanderhoek (2010) |
| 2008 | Blood | 10 | 7.1-10 | 265-370 (334) | Buck (2008) |
| 2014 | GI | 21 | 5–7 | 185–259 | Hoh (2014) |
| 2011 | GI | 21 | 0.1/kg | 3.7/kg | Kameyama (2011) |
| 2010 | GI | 21 | 8.1-10.8 | 300–400 | Yue (2010) |
| 2009 | GI | 21 | 0.18 | 3.5 /Kg | Kameyama (2009) |
| 2008 | GI | 5 | 8.7-12.7 | 328-470 | Roels (2008) |
| 2018 | Gastric | 19 | 8.3<br>8.02-8.6 | Mean=306.6<br>296.7–317.6 | Honma (2018) |

| Year | Organ system | N | mCi injected (mean) | MBq Injected (mean) | Reference |
|---|---|---|---|---|---|
| 2016 | Gastric | 17 | 0.1/kg | 3.7/kg | Nakajo (2016) |
| 2016 | Gastric | 96 | 9.5 | 350 | Staniuk (2016) |
| 2016 | Gastric | 10 | 5.6 ± 0.3 | 208.2 ± 10.4 | Sharma (2016) |
| 2015 | Gastric | 64 | 0.2/kg | 7.4/kg | Wang (2015) |
| 2013 | Gastric | 104 | 9.5 ± 0.5 | 350 ± 20 | Malkowski (2013) |
| 2011 | Gastric | 45 | 7.3-9.2 | 270-340 | Ott (2011) |
| 2007 | Gastric | 45 | 7.3-9.2 | 270-340 | Herrmann (2007) |
| 2020 | Brain | 81 | 3.8-10.7<br>Mean= 8.2±1.2 | 141–398<br>(mean, 302 ± 45.2 | Ogawa (2020) |
| 2020 | Brain | 17 | 9.2-10.05 | 340–372 | Bashir (2020) |
| 2020 | Brain | 43 | 9.5 | 353 | Bashir (2020) |
| 2019 | Brain | 14 | 8.4-11.3 | 310–420 MBq | Nikaki (2019) |
| 2019 | Brain | 20 | 0.13 | 5 | Berro (2019) |
| 2019 | Brain | 13 | 0.07/kg<br>9.4 ± 1.3 | 2.6/kg<br>350 ± 50 | Fernandez (2019) |
| 2018 | Brain | 30 | 5.4 | 200 | Brahm (2018) |
| 2017 | Brain | 27 | 0.07/Kg | 2.6/kg | Holdhoff (2017) |
| 2016 | Brain | 39 | 8.8 ± 1.04 | 317.1 ± 38.5 | Kudomi (2016) |
| 2016 | Brain | 55 | 2.9-10.6<br>mean, 7.7 ± 1.6 | 106-393<br>mean, 285 ± 58 | Lin (2016) |
| 2016 | Brain | 37 | 0.1/kg | 3.7/kg | Mitamura (2016) |
| 2016 | Brain | 10 | 0.07/kg | 2.6/kg | Lodge (2016) |
| 2015 | Brain | 12 | 5.3 | 195 | Blanchet (2015) |
| 2015 | Brain | 26 | 0.054/kg | 2.0/kg | Ferdova (2015) |
| 2015 | Brain | 19 | 10.1±1.0 | 374.2±36.7 | Zhao (2015) |
| 2015 | Brain | 39 | 0.14/kg | 5.0/kg | Collett (2015) |
| 2014 | Brain | 41 | 4.4–8.7 | 161-323 | Belohlavek (2014) |
| 2014 | Brain | 23 | 3.7-6.2 | 138–230 | Nowosielski (2014) |

| Year | Organ system | N | mCi injected (mean) | MBq Injected (mean) | Reference |
|---|---|---|---|---|---|
| 2014 | Brain | 56 | 0.1/kg | 3.7/kg | Zhao (2014) |
| 2013 | Brain | 21 | 7.5±72 | 279±72 | Shinomiya (2013) |
| 2012 | Brain | 15 | 10 | 370 | Enslow (2012) |
| 2012 | Brain | 24 | 0.03-0.18/kg | 1.1-6.6/kg | Harris (2012) |
| 2012 | Brain | 26 | 5.97 | 221 | Idema (2012) |
| 2012 | Brain | 20 | 10 | 370 | Jeong (2012) |
| 2012 | Brain | 2 | 5 | 185 | Laymon (2012) |
| 2012 | Brain | 56 | 0.1/kg | 3.7/kg | Yamamoto (2012) |
| 2009 | Brain | 15 | 0.06/kg | 2.1 /kg | Tripathi (2009) |
| 2009 | Brain | 14 | 5.4 | 200 | Price (2009) |
| 2008 | Brain | 13 | 8.7 | 322±85 | Ullrich (2008) |
| 2007 | Brain | 21 | 0.05/kg | 2.0/kg | Chen (2007) |
| 2007 | Brain | 9 | 0.04/kg | 1.5/kg | Schiepers (2007) |
| 2008 | Brain | 41 | Mean 4.35<br>3.49-6.38 | Mean 161<br>129-236 | Hatakeyama (2008) |
| 2008 | Brain | 12 | Mean 4.74<br>4.16-5.19 | Mean 175<br>154-192 | Spence (2008) |
| 2006 | Brain | 12 | 5 | 185 | Muzi (2006) |
| 2006 | Brain | 10 | Mean 4.0<br>2.8-5.4 | Mean 150<br>104-202 | Yamamoto (2006) |
| 2006 | Brain | 25 | 10 | 370 | Saga (2006) |
| 2005 | Brain | 25 | Mean: 4.7<br>3.8-5.9 | Mean 174<br>141-218 | Chen (2005) |
| 2005 | Brain | 26 | 10 | 370 | Choi (2005) |
| 2005 | Brain | 25 | Mean 8.7<br>3.0-10.0 | Mean 322<br>111-370 | Jacobs (2005) |
| 2020 | Breast | 44 | 10 | 370 | Wesolowski (2020) |
| 2019 | Breast | 16 | 8.7 | 324 | Ueberroth (2019) |
| 2019 | Breast | 85 | 0.08 or 0.13 | 3/kg or 5/kg | Lovinfosse (2019) |
| 2017 | Breast | 13 | 5.9 | 220 | Palmieri (2017) |

| Year | Organ system | N | mCi injected (mean) | MBq Injected (mean) | Reference |
|---|---|---|---|---|---|
| 2016 | Breast | 10 | | | O'Sullivan (2016) |
| 2015 | Breast | 15 | 0.095/kg | 3.5/kg | Crippa (2015) |
| 2015 | Breast | 43 | 3.0-5.5 | 110-204 | Kostakoglu (2015) |
| 2014 | Breast | 15 | 4.1-10.3 | 153 – 381 | Veronese (2014) |
| 2014 | Breast | 28 | 0.07/kg | 2.59/kg | Wang (2014) |
| 2014 | Breast | 30 | 10.4±1.5 | 385 ± 56 | Marti-Climent (2014) |
| 2014 | Breast | 20 | 0.095/kg | 3.5/kg | Woolf (2014) |
| 2013 | Breast | 15 | 4.1-10.3 | 153-381 | Willaime (2013) |
| 2012 | Breast | 5 | 5.4 | 200 | Contractor (2012) |
| 2012 | Breast | 15 | 10 | 370 | Lubberink (2012) |
| 2011 | Breast | 21 | 3.9-5.9 (5.4) | 145-218 (200) | Contractor (2011) |
| 2007 | Breast | 15 | 4.1-10.3 | 153-381 | Kenny (2007) |
| 2006 | Breast | 10 | 4.3-11.3 | 160-420 | Been (2006) |
| 2005 | Breast | 15 | 4.1-10.5 | 153-389 | Kenny (2005) |
| 2005 | Breast | 14 | 3.5 | 130 | Pio (2005) |
| 2004 | Breast | 12 | 8.1-12.1 | 300-450 | Smyczek-Gargya (2004) |
| 2018 | Oral Cancer | 36 | 0.049 | 1.8/kg | Baxa (2018) |
| 2013 | Periampullary | 21 | 7.2-10 | 265-370 | Cheng (2013) |
| 2018 | Pancreas | 27 | 8.1 | 300 | Wieder (2018) |
| 2017 | Pancreas | | 5.03 to 8.73 Mean, 6.21 | 186 to 324 Mean, 230 MBq | Pretz (2017) |
| 2016 | Pancreas | 15 | 0.1/kg | 3.7/kg | Nakajo (2016) |
| 2016 | Pancreas | 6 | 10.1±1.0 | 374.2±36.7 | Debebe (2016) |
| 2015 | Pancreas | 7 | 10 ±1 | 370 ± 37 | Goryawala (2015) |
| 2015 | Pancreas | 20 | Mean 5.6 | Mean 208.2 | Challapalli (2015) |
| 2012 | Pancreas | 46 | 8.1 | 300 | Herrmann (2012) |
| 2008 | Pancreas | 31 | 7.3-9.2 | 270-340 | Herrmann (2008) |
| 2008 | Pancreas | 5 | 5.2-7 | 192-259 | Quon (2008) |

| Year | Organ system | N | mCi injected (mean) | MBq Injected (mean) | Reference |
|---|---|---|---|---|---|
| 2019 | Lymphoma | 52 | 10 | 370 | Zanoni (2019) |
| 2018 | Lymphoma | 44 | 0.10 | 3.7 | Wang (2018) |
| 2016 | Lymphoma | 65 | 8.0 ± 0.8 | 296 ± 30 | Schoder (2016) |
| 2016 | Lymphoma | 8 | 0.14/kg | 5.2/kg | Constantini (2016) |
| 2016 | Lymph Nodes | 70 | 10 | 370 | Rayamajhi (2016) |
| 2015 | Lymphoma | 65 | 8±0.8 | 296 ± 30 | Schoder (2015) |
| 2015 | Lymphoma | 26 | 5 | 185 | Wondergem (2015) |
| 2014 | Lymphoma | 21 | 2.7-5.0 | 99.9-185 | Mena (2014) |
| 2014 | Lymphoma | 22 | 5 | 185 | Wondergem (2014) |
| 2014 | Lymphoma | 61 | 8.8-12 | 326–444 | Lee (2014) |
| 2014 | Lymphoma | 54 | 7.3-9.2 | 270-340 | Hermann (2014) |
| 2007 | Lymphoma | 22 | Mean 8.11<br>7.20-9.19 | Mean 300<br>270-340 | Herrmann (2007) |
| 2007 | Lymphoma | 48 | 3.9 | 148.6 | Kasper (2007) |
| 2006 | Lymphoma | 34 | Mean 9.3<br>7.1-10 | Mean 345<br>265-370 | Buck (2006) |
| 2004 | Lymphoma | 7 | 4.3 - 13.2 | Mean = 324<br>159 - 489 | Buchmann (2004) |
| 2003 | Lymphoma | 11 | 7.5 | 280 | Wagner (2003) |
| 2020 | Melanoma | 5 | 5 | 185 | Yeh (2020) |
| 2107 | Melanoma | 25 | | | Heil (2017) |
| 2015 | Melanoma | 5 | 4.3-5.3 | 160–195 | Algazi (2015) |
| 2010 | Melanoma | 12 | 5.3 mCi +/- 10% | 196.1 MBq +/- 10% | Ribas (2010) |
| 2003 | Melanoma | 10 | 10.8 | Med= 400<br>185-430 | Cobben (2003) |
| 2019 | Colorectal | 68 | 0.07 | 2.6/kg | Kim (2019) |
| 2017 | Colorectal | 39 | 9.5 | 350 | Mogensen (2017) |
| 2017 | Colorectal | 32 | 0.1/kg | 3.7/kg | Nakajo (2017) |
| 2014 | Colorectal | 30 | 0.1/kg | 3.7/kg | Nakajo (2014) |

| Year | Organ system | N | mCi injected (mean) | MBq Injected (mean) | Reference |
|---|---|---|---|---|---|
| 2013 | Colorectal | 18 | 4.3<br>3.5-5.0 | Mean 159.1<br>111-185 | Hong (2013) |
| 2013 | Colorectal | 28 | 0.1/kg | 3.7/kg | Nakajo (2013) |
| 2004 | Colorectal | 18 | 9.7 | 360 ± 25 | Visvikis (2004) |
| 2003 | Colorectal | 10* | 9.5 | 351 ± 52 | Francis (2003) |
| 2003 | Colorectal | 17 | Mean 9.7<br>8.4-11.1 | Mean=360<br>312-412 | Francis (2003) |
| 2015 | Rectal | 5 | 5 | 185 | Manning (2015) |
| 2015 | Rectal | 20 | 0.11/kg | 4/kg | Rendl (2015) |
| 2013 | Rectal | 14 | 10 | 370 | Dehdashti (2013) |
| 2011 | Rectal | 9 | 2.9-11.2<br>(5.5) | 109-416<br>(205) | Muijs (2011) |
| 2007 | Rectal | 10 | 8.1 | 300 | Wieder (2007) |
| 2019 | Bone Marrow | 25 | 5.4 | 200 | Tsujikawa (2019) |
| 2018 | Bone Marrow | 23 | 0.07/kg<br>Max=3.00/kg | 2.59/kg<br>Max=111/kg | Williams (2018) |
| 2017 | Bone Marrow | 15 | 0.08/kg | 3/kg | Vercellino (2017) |
| 2016 | Bone Marrow | 16 | 0.12/kg | 4.5/kg | Wyss (2016) |
| 2012 | Bone marrow | 1 | | | Zade (2012) |
| 2011 | Bone Marrow Pelvic | 2 | 0.07/kg<br>Max=5 | 2.6/kg<br>Max=185 | McGuire (2011) |
| 2011 | Bone marrow | 17 | 10.8 | 400 | Agool (2011) |
| 2010 | Bone marrow | 1 | | | Agool (2010) |
| 2006 | Bone marrow | 18 | 10.8 | 400 | Agool (2006) |
| 2008 | Bone & soft tissue | 22 | 9.5-11.5 | 350-425 | Buck (2008) |
| 2004 | Soft tissue | 19 | 10.8 | Mean=400<br>115 -430 | Cobben (2004) |
| 2020 | Sarcoma | 15 | 4.96–9.72 | 184-360 | Kairemo (2020) |

| Year | Organ system | N | mCi injected (mean) | MBq Injected (mean) | Reference |
|---|---|---|---|---|---|
| 2012 | Sarcoma | 20 | 5.7-8.1 (6.6±0.5) | 210.9-299.7 (244.2±0.5) | Benz (2012) |
| 2007 | Sarcoma | 10 | Mean 9.81 3.24-11.62 | Mean 363 120-430 | Been (2007) |
| 2020 | Head & Neck | 41 | 0.2/kg | 7.4/kg | Hu (2020) |
| 2019 | Head & Neck | 36 | 4.9±2.03 | 180±75 | Cegla (2019) |
| 2015 | Head & Neck | 10 | | | Nyflot (2015) |
| 2015 | Head & Neck | 22 | 2.2 | 80 | Vojitsek (2015) |
| 2014 | Head & Neck | 32 | 0.1/kg | 3.7/kg | Hoshikawa (2014) |
| 2014 | Head & Neck | 5 | 0.07/kg | 2.59/kg | Liu (2014) |
| 2013 | Head/Neck | 46 | 6.76 | 250 | Arens (2013) |
| 2013 | Head/Neck | 48 | 6.8 | 250 | Hoeben (2013) |
| 2013 | Head/Neck | 30 | 0.09/kg | 3.5/kg | Hoshikawa (2013) |
| 2012 | Head/Neck | 23 | 0.09/kg | 3.5/kg | Hoshikawa (2012) |
| 2012 | Head/Neck | 13 | 8.1 | 300 | Inubushi (2012) |
| 2012 | Head/Neck | 28 | 0.09/kg | 3.5/kg | Kishino (2012) |
| 2011 | Head/Neck | 10 | 0.07/kg Max=5 | 2.6/kg Max=185 | McGuire (2011) |
| 2010 | Head/Neck | 10 | | 250 | Troost (2010) |
| 2007 | Head/Neck | 10 | 6.76 | 250 | Troost (2007) |
| 2004 | Head/Neck | 21 | 9.2 | Mean=340 165-650 | Cobben (2004) |
| 2012 | Head/Neck | 8 | 0.07/kg | 2.6/kg | Larsson (2012) |
| 2010 | Germ Cell Tumors | 11 | 9.5-10.8 | 350 - 400 | Pfannenberg (2010) |
| 2018 | Esophagus | 5 | 10 | 370 | Gerbaudo (2018) |
| 2015 | Esophagus | 36 | 8.1-10.8 | 300-400 | Ma (2015) |
| 2015 | Esophagus | 10 | 8.1-10.8 | 300-400 | Zhang (2015) |
| 2015 | Esophagus | 100 | 10-20 | 370–740 | Ma (2015) |
| 2014 | Esophagus | 34 | 9.2-12.2 | 340-450 | Chen (2014) |
| 2012 | Esophagus | 22 | 8.1-10.8 | 300-400 | Han (2012) |

| Year | Organ system | N | mCi injected (mean) | MBq Injected (mean) | Reference |
|---|---|---|---|---|---|
| 2011 | Esophagus | 22 | 8.1-10.8 | 300-400 | Han (2011) |
| 2005 | Esophagus | 10 | Mean 11.0<br>9.2-12-2 | Mean 410<br>340-450 | Van Westreenen (2005) |
| 2018 | Various Solid | 14 | 9.8 | 362 | Scarpelli (2018) |
| 2016 | Various Solid | 46 | 3.4–5.4<br>Mean, 4.4 ± 0.4 | 126–200<br>Mean, 164 ± 15 | Minamimoto (2016) |
| 2015 | Various Solid | 20 | | | Bruce (2015) |
| 2013 | Various Solid | 16 | ~6.5 | ~240 | Vanderhoek (2013) |
| 2016 | Various | 100 | 0.14/kg | 5.0/kg | Johnbeck (2016) |
| 2016 | Various | 15 | 9.4–10.5<br>Mean 10.1 | 347–389<br>Mean 372 | McHugh (2016) |
| 2015 | Various | 20 | 6.6-10.3 | 245-382 | Ye (2015) |
| 2012 | Various | 4 | 6.76 | 250 | Desar (2012) |
| 2003 | Various | 18 | 5.0 | 185 max | Vesselle (2003) |
| 2010 | Various | 13 | 0.12/kg | 4.5/kg | Hayman (2010) |
| 2005 | Various | 33 | Mean 9.5<br>8.4-9.7 | Mean 350<br>310-360 | Shields (2005) |
| | **Total No. Subjects:** | **6150**** | | | |

*Papers marked with an asterisk in the "N" column were not counted towards the total as they could not be verified as unique with certainty.

**The total number in the last row of the "N" column of Table 13 represents a conservative statement of apparently unique subjects.

As is evident from the information in Table 9, many of the published studies did not specifically mention the specific activity of the [F-18]FLT or provide sufficient information to calculate it so it is not possible to actually assess the amount of FLT that was actually administered to the patient. This amount could be estimated if needed as most studies cite the method of synthesis and all of them are using no carrier added (nca) nucleophilic synthetic methods that give high specific activity. In addition, only the Turcotte (2008) and Spence (2008) papers specifically address safety issues by describing laboratory results post injection or assess for neurological sequelae such as mild peripheral neuropathy. This is addressed in Section 6 where two studies with safety monitoring are detailed. However, the majority of these publications did indicate

that IRB or Ethics Committee approval was obtained for the study, so the patients would have been observed for clinically evident adverse events, none of which were reported.

## VIII. REFERENCES

Agool A, Dierckx RAJO, de Wolf JTM, Vellenga E, Slart RHJA. Extramedullary haematopoiesis imaging with 18F-FLT PET. European Journal of Nuclear Medicine and Molecular Imaging. 2010; 37:1620.

Agool A, Schot BW, Jager PL, Vellenga E. 18F-FLT PET in hematologic disorders: A novel technique to analyze the bone marrow compartment. Journal of Nuclear Medicine. 2006; 47(10):1592-1598.

Agool A, Slart RH, Kluin PM, de Wolf JT, Dierckx RA, Vellenga E. F-18 FLT PET: A noninvasive diagnostic tool for visualization of the bone marrow compartment in patients with aplastic anemia. Clin Nucl Med. 2011; 36(4):286-9.

Algazi A, Cha E, Ortiz-Urda S, et al. The combination of axitinib followed by paclitaxel/carboplatin yields extended survival in advanced BRAF wild-type melanoma: results of a clinical/correlative prospective phase II clinical trial. British Journal of Cancer. 2015; 112: 1326-1331.

American College of Toxicology. Final report on the safety assessment of benzyl alcohol, benzoic acid, and sodium benzoate. International Journal of Toxicology. 2001; 20(3 suppl):23-50.

Arens AI, Troost EG, Hoeben BA, et al. Semiautomatic methods for segmentation of the proliferative tumour volume on sequential FLT PET/CT images in head and neck carcinomas and their relation to clinical outcome. Eur J Nucl Med Mol Imaging, 2013.

Bading JR, Shields AF. Imaging of cell proliferation: Status and prospects. Journal of Nuclear Medicine. 2008; 49, No. 6 suppl.:64-80s.

Bashir A, Vestergaard, M, Marner L, et al. PET Imaging of Meningioma With 18F-FLT: A Predictor of Tumour Progression. BRAIN. 2020; 143: 3308–3317.

Bashir A, Binderup T, Vestergaard M, et al. In Vivo Imaging of Cell Proliferation in Meningioma Using 3'-Deoxy-3'-[18F]Fluorothymidine PET/MRI. European Journal of Nuclear Medicine and Molecular Imaging. 2020; 47:1496–

Baxa J, Ferda J, Ferdova E Hybrid, et al. Imaging PET/CT with Application of 18F-Fluorothymidine in Patients with Head and Neck Carcinoma Undergoing Radiotherapy. Anticancer Research. 2018; 38: 4153-4157.

Beauregard J, Giraudet A, Aide N, et al. Evaluation of a new visual uptake scoring scale for 18F-fluorothymidine positron emission tomography in the diagnosis of pulmonary lesions. Nucl Med Comm. 2013; 34(6).

Been LB, Elsinga PH, de Vries J, et al. Positron emission tomography in patients with breast cancer using 18F-3'-deoxy-3'-fluoro-l-thymidine 18F-FLT)-a pilot study. European Journal of Surgical Oncology. 2006; 32(1):39-43.

Been LB, Suurmeijer AJH, Elsinga PH, et al. 18F-fluorodeoxythymidine PET for evaluating the response to hyperthermic isolated limb perfusion for locally advanced soft-tissue sarcomas. Journal of Nuclear Medicine. 2007; 48(3):367-372.

Belohlavek O, Fencl P, Majovsky M, et al. FLT-PET in previously untreated patients with low-grade glioma can predict their overall survival. Nuclear Medicine Review. 2014; 17(1): 7–12.

Benz MR, Czernin J, Allen-Auerbach MS, et al. 3'-deoxy-3'-[18F]fluorothymidine positron emission tomography for response assessment in soft tissue sarcoma: a pilot study to correlate imaging findings with tissue thymidine kinase 1 and Ki-67 activity and histopathologic response. Cancer. 2012; 118(12):3135-44.

Berro D, Collet S, Constans J, et al. Comparison between MRI-derived ADC maps and 18FLT-PET in pre-operative glioblastoma. Journal of Neuroradiology. 2019; 46:359–366.

Bhoil A, Singh B, Singh N, et al. Can 3'-deoxy-3'-18F-fluorothymidine or 2'-deoxy-2'-18F-fluoro-d-glucose PET/CT better assess response after 3-weeks treatment by epidermal growth factor receptor kinase inhibitor, in non-small lung cancer patients? Preliminary results. Hellenic Journal of Nuclear Medicine. 2014; 17(2): 90-96.Blanchet E, Taieb D, Millo C, et al. 18F-FLT PET/CT in the evaluation of pheochromocytomas and paragangliomas: a pilot study. J Nucl Med. 2015; 56: 1849–1854.

Brahm C, Hollander M, Enting R, et al. Serial FLT PET imaging to discriminate between true progression and pseudoprogression in patients with newly diagnosed glioblastoma: a long-term follow-up study. European Journal of Nuclear Medicine and Molecular Imaging. 2018; 45:2404–2412.

Brockenbrough JS, Souquet T, Morihara JK, et al. Tumor 3'-deoxy-3'-18F-fluorothymidine 18F-FLT uptake by PET correlates with thymidine kinase 1 expression: static and kinetic analysis of 18F-FLT PET studies in lung tumors. J Nucl Med. 2011; 52:1181–1188.

Bruce J, Scully P, Carmichael L, et al. Pharmacodynamic study of axitinib in patients with advanced malignancies assessed with 18F-3'deoxy-3'fluoro-l-thymidine positron emission tomography/computed tomography. Cancer Chemother Pharmacol. 2015; 76: 187–195.

Buchmann I, Neumaier B, Schreckenberger M, Reske S. [18F]3'-Deoxy-3'-fluorothymidine-PET in NHL patients: Whole-body biodistribution and imaging of lymphoma manifestations-a pilot study. Cancer Biotherapy & Radiopharmaceuticals. 2004; 19(4):436-442.

Buck AK, Bommer M, Juweid ME, et al. First demonstration of leukemia imaging with the proliferation marker 18F-flurodeoxythymidine. Journal of Nuclear Medicine. 2008; 49(11):1756-1762.

Buck AK, Bommer M, Stilgenbauer S, et al. Molecular imaging of proliferation in malignant lymphoma. Cancer Research. 2006; 66(22):11055-11061.

Buck AK, Halter G, Schirrmeister H, et al. Imaging proliferation in lung tumors with PET: 18F-FLT versus 18F-FDG. Journal of Nuclear Medicine. 2003; 44(9):1426-1431.

Buck AK, Herrmann K, zum Buschenfelde CM, et al. Imaging bone and soft tissue tumors with the proliferation marker [18F] fluorodeoxythymidine. Clinical Cancer Research. 2008; 14(10):2970-2977.

Buck AK, Hetzel M, Schirrmeister H, et al. Clinical relevance of imaging proliferative activity in lung nodules. European Journal of Nuclear Medicine and Molecular Imaging. 2005; 32(5):525-533.

Buck AK, Schirrmeister H, Hetzel M, et al. 3-deox-3-[18F] fluorothymidine-positron emission tomography for noninvasive assessment of proliferation in pulmonary nodules. Cancer Research. 2002; 62(12):3331-3334.

Center for Drug Evaluation and Research. Ammonul Injection, NDA 20-645, Product Labeling, Approved 2/17/2005.

Cegła P, Burchardt E, Cholewiński W, et al. Comparison of Semiquantitative Metabolic Parameters of the Primary Tumor Obtained in PET/CT with 18F-FDG and 18F-FLT in Patients with Cervical Cancer. Nuklearmedizin. 2020; 59: 241–247.

Cegla P, Joanna K, Sebastian G, et al. Correlation between tumour biology status measured in triple-tracer 18F-fluorodeoxyglucose– 18F-fluorothymidine–18F-fluoromisonidazole-PET/CT study and human papillomavirus status in patients with head and neck cancer. Nuclear Medicine Communications. 18 March 2019.

Challapalli A, Barwick T, Pearson R, et al. 3'-Deoxy-3'-18F-fluorothymidine positron emission tomographyas an early predictor of disease progression in patients with advanced and metastatic pancreatic cancer. Eur J Nucl Med Mol Imaging. 2015; 42: 831–840.

Channing MA, Huang BX, Eckelman WC. Analysis of residual solvents in 2-[18F]FDG by GC. Nuclear Medicine and Biology. 2001; 28(4):469-471.

Cheng MF, Wang HP, Tien YW, et al. Usefulness of PET/CT for the differentiation and characterization of periampullary lesions. Clin Nucl Med. 2013; 38(9):703-708.

Chen X, Zhao X, Gao Z, et al. Proliferation PET image to characterize pathological spatial features in patients with non-small cell lung cancer: a pilot study. Int J Clin Exp Med. 2015; 8(6): 9758-9764.

Chen H, Li Y, Wu H, et al. 3'-Deoxy-3'-[18F]-fluorothymidine PET/CT in early determination of prognosis in patients with esophageal squamous cell cancer. Comparison with [18F]-FDG PET/CT. Strahlenther Onkol. 2015; 191: 141–152.

Chen W, Cloughesy T, Kamdar N, et al. Imaging proliferation in brain tumors with 18F-FLT PET: comparison with 18F-FDG. Journal of Nuclear Medicine. 2005; 46(6):945-952.

Chen W, Delaloye S, Silverman DHS, et al. Predicting treatment response of malignant gliomas to bevacizumab and irinotecan by imaging proliferation with [18F] fluorothymidine positron emission tomography: A pilot study. Journal of Clinical Oncology. 2007; 25(30):4714-4721.

Choi SJ, Kim JS, Kim JH, et al. [18F]3'-deoxy-3'-fluorothymidine PET for the diagnosis and grading of brain tumors. European Journal of Nuclear Medicine and Molecular Imaging. 2005; 32(6):653-659.

Cho L, Kim C, Viswanathan A. Pilot study assessing 18F-fluorothymidine PET/CT in cervical and vaginal cancers before and after external beam radiation. Gynecologic Oncology Reports. 2015; (14): 34–37.

Chopra S, Engineer R, Shah S, et al. MRI- and PET-Guided Interstitial Brachytherapy for Postsurgical Vaginal Recurrences of Cervical Cancer: Results of Phase II Study. Int J Radiation Oncol Biol Phys. 2020; 106(2): 310e319.

Christensen T, Langer S, Persson G. 18F-FLT-PET/CT Adds Value to 18F-FDG-PET/CT for Diagnosing Relapse After Definitive Radiotherapy in Patients with Lung Cancer. Results of A Prospective Clinical Trial. Journal of Nuclear Medicine. Published on October 9, 2020.

Cobben DCP, Elsinga PH, Suurmeijer AJH, et al. Detection and grading of soft tissue sarcomas of the extremities with 18F-3'-fluoro-3'-eoxy-l-thymidine. Clinical Cancer Research. 2004; 10(5):1685-1690.

Cobben DCP, Jager PL, Elsinga PH, et al. 3'-18F-fluoro-3'-deoxy-l-thymidine: A new tracer for staging metastatic melanoma? Journal of Nuclear Medicine. 2003; 44(12):1927-1932.

Cobben DCP, van der Laan BFAM, Maas B, et al. 18F-FLT PET for visualization of laryngeal cancer: Comparison with 18F-FDG PET. Journal of Nuclear Medicine. 2004; 45(2):226-231.

Collet S, Valable S, Constans J, et al. [18F]-fluoro-L-thymidine PET and advanced MRI for preoperative gradingof gliomas. NeuroImage: Clinical. 2015; 8: 448–454.

Contractor K, Aboagye EO, Jacob J, Challapalli A, Coombes RC, Stebbing J. Monitoring early response to taxane therapy in advanced breast cancer with circulating tumor cells and [18F] 3´-deoxy-3´-fluorothymidine PET: a pilot study. Biomark Med. 2012; 6(2):231-3.

Contractor K, Challapalli A, Tomasi G, et al. Imaging of cellular proliferation in liver metastasis by [18F]fluorothymidine positron emission tomography: effect of therapy. Phys Med Biol. 2012; 7;57(11):3419-33.

Contractor KB, Kenny LM, Stebbing J, et al. Biological basis of [$^{11}$C]choline-positron emission tomography in patients with breast cancer: comparison with [$^{18}$F]fluorothymidine positron emission tomography. Nucl Med Commun. 2011; 32(11):997-1004.

Costantini D, Vali R, McQuattie S, et al. A Pilot study of 18F-FLT PET/CT in pediatric lymphoma. International Journal of Molecular Imaging. 2016.

Crandall J, Tahari A, Juergens R, et al. A comparison of FLT to FDG PET/CT in the early assessment of chemotherapy response in stages IB–IIIA resectable NSCLC. EJNMMI Research. 2017; 7(8).

Crippa F, Agresti R, Sandri M, et al. 18F-FLT PET/CT as an imaging tool for early prediction of pathological response in patients with locally advanced breast cancer treated with neoadjuvant chemotherapy: a pilot study. Eur J Nucl Med Mol Imaging. 2015; 42: 818–830.

Crump M. Hitting the target in MCL. Blood, 2012 May 17;119(20):4580-1.

Cysouw M, Golla S, Frings V, et al. Partial-volume correction in dynamic PET-CT: effect on tumor kinetic parameter estimation and validation of simplified metrics. EJNMMI Research. 2019; 9:12.

Debebe S, Goryawala M, Adjouadi M, Mcgoron A, and Güleç S. 18F-FLT positron emission tomography/computed tomography imaging in pancreatic cancer: determination of tumor proliferative activity and comparison with glycolytic activity as measured by 18F-FDG positron emission tomography/computed tomography imaging. Mol Imaging Radionucl Therp. 2016; 25: 32-38.

Dehdashti F, Grigsby PW, Myerson RJ, Nalbantoglu I, Ma C, Siegel BA. Positron emission tomography with [18F]-3'-deoxy-3'fluorothymidine (FLT) as a predictor of outcome in patients with locally advanced resectable rectal cancer: a pilot study. Mol Imaging Biol. 2013; (1):106-13.

de Langen AJ, Klabbers B, Lubberink M, et al. Reproducibility of quantitative 18F-3'-deoxy-3'-fluorothymidine measurements using positron emission tomography. European Journal of Nuclear Medicine and Molecular Imaging. 2009; 36(3):389-395.

Desar IM, Gilles R, van Herpen CM, et al. 18F-FLT-PET for response evaluation of MEK inhibitor selumetinib (AZD6244, ARRY-142886) in patients with solid tumors. World J Nucl Med. 2012; 11(2):65-9.

Dittmann H, Dohmen BM, Kehlbach R, et al. Early changes in [18F]FLT uptake after chemotherapy: An experimental study. European Journal of Nuclear Medicine and Molecular Imaging. 2002; 29(11):1462-1469.

Dittmann H, Dohmen BM, Paulsen F, et al. [18F]FLT PET for diagnosis and staging of thoracic tumours. European Journal of Nuclear Medicine and Molecular Imaging. 2003; 30(10):1407-1412.

Dreisbach RH, Robertson WO. Handbook of poisoning: Prevention, diagnosis and treatment. Appleton and Lange Publ, Los Altos (CA). 1987; 12:171-174.

Enslow MS, Zollinger LV, Morton KA, et al. Comparison of F-18 fluorodeoxyglucose and F-18 fluorothymidine positron emission tomography in differentiating radiation necrosis from recurrent glioma. Clin Nucl Med. 2012; 37(9):854-61.

Everitt S, Ball D, Hicks R, et al. Prospective study of serial Imaging comparing fluorodeoxyglucose positron emission tomography (PET) and fluorothymidine PET during radical chemoradiation for non-small cell lung cancer: reduction of detectable proliferation associated with worse survival. Int J Radiat Oncol Biol Phys. Epub July 24, 2017.

Everitt S, Ball D, Hicks R, et al. Differential 18F-FDG and 18F-FLT Uptake on serial PET/CT imaging before and during definitive chemoradiation for non–small cell lung cancer. J Nucl Med. 2014; 55:1069–1074.

Faraj A, Fowler DA, Bridges EG, Sommadossi JP. Effects of 2',3'-dideoxynucleosides on proliferation and differentiation of human pluripotent progenitors in liquid culture and their effects on mitochondrial DNA synthesis. Antimitcrobial Agents and Chemotherapy. 1994; 38(5):924-930.

Ferdova E, Ferda J, Baxa J, et al. Assessment of grading in newly-diagnosed glioma using 18F-Fluorothymidine PET/CT. Anticancer Research. 2015; 35: 955-960.

Fernandez P, Zanotti-Fregonara P, Eimer S, et al. Combining 3'-Deoxy-3'-[18F] fluorothymidine and MRI increases the sensitivity of glioma volume detection. Nucl Med Commun. 7 June 2019.

Flexner C, van der Horst C, Jacobson MA, et al. Relationship between plasma concentrations of 3'-deoxy-3'-fluorothymidine (Alovudine) and antiretroviral activity in two concentration-controlled trails. Journal of Infectious Diseases. 1994; 170(6):1394-1403.

Francis DL, Freeman A, Visvikis D, et al. In vivo imaging of cellular proliferation in colorectal cancer using positron emission tomography. Gut. 2003; 52(11):1602-1606.

Francis DL, Visvikis D, Costa DC, et al. Potential impact of [18F]3'-deoxy-3'-fluorothymidine versus [18F]fluoro-2-deoxy-d-glucose in positron emission tomography for colorectal cancer. European Journal of Nuclear Medicine and Molecular Imaging. 2003; 30(7):988-994.

Frings V, Yaqub M, Hoyng L, et al. Assessment of simplified methods to measure 18F-FLT uptake changes in EGFR-mutated non–small cell lung cancer patients undergoing EGFR tyrosine kinase inhibitor treatment. J Nucl Med. 2014; 55: 1417–1423.

Frings V, de Langen AJ, Yaqub M, et al. Methodological Considerations in Quantification of 3'-Deoxy-3'-[18F]Fluorothymidine Uptake Measured with Positron Emission Tomography in Patients with Non-Small Cell Lung Cancer. Mol Imaging Biol. 2014; 16:136-145.

Frings V, van der Veldt AA, Boellaard R, et al. Pemetrexed induced thymidylate synthase inhibition in non-small cell lung cancer patients: A pilot study with 3'-deoxy-3'-[18F]fluorothymidine positron emission tomography. PLoS One. 2013; 24;8(5).

Gerbaudo V, Killoran J, Kim C, et al. Pilot study of serial FLT and FDG-PET/CT imaging to monitor response to neoadjuvant chemoradiotherapy of esophageal adenocarcinoma: correlation with histopathologic response. Annals of Nuclear Medicine. 2018; 32:165–174.

Ghosn J, Wuinson A, Sabo N, et al. Antiviral activity of low-dose alovudine in antiretroviral-experienced patients: results from a 4-week randomized, double-blind, placebo-controlled dose-ranging trial. HIV Medicine. 2007; 8:142-147.

Goryawala M, Adjoua M, Gulec S. Proliferative and glycolytic assessment of the whole-body bone marrow compartment. Molecular Imaging and Radionuclide Therapy. 2015; 24(2): 71-79.

Grierson JR, Shields AF. Radiosynthesis of 3'-deoxy-3'-[18F]fluorothymidine: [18F]FLT for imaging of cellular proliferation in vivo. Nuclear Medicine and Biology. 2000; 27(2):143-156.

Hackett SL, Liu D, Chalkidou A, Marsden P, Landau D, Fenwick JD. Estimation of input functions from dynamic [18F]FLT PET studies of the head and neck with correction for partial volume effects. EJNMMI Res. 2013; 3:84.

Halter G, Buck AK, Schirrmeister H, et al. [18F] 3-deoxy-3'-fluorothymidine positron emission tomography: alternative or diagnostic adjunct to 2-[18F]-fluoro-2-deoxy-D-glucose positron

emission tomography in the workup of suspicious central focal lesions? Journal of Thoracic and Cardiovascular Surgery. 2004; 127(4):1093-1099.

Han E, Lee B, Park Y and Choi W. Early assessment of response to induction therapy in acute myeloid leukemia using 18F-FLT PET/CT. EJNMMI Research. 2017; 7(75).

Han D, Yu J, Zhong X, Fu Z, et al. Comparison of the diagnostic value of 3'-deoxy-3'-18F-fluorothymidine and 18F-fluorodeoxyglucose positron emission tomography/computed tomography in the assessment of regional lymph node in thoracic esophageal squamous cell carcinoma: A pilot study. Dis Esophagus. 2012; 25(5):416-26.

Harris RJ, Cloughesy TF, Pope WB, et al. 18F-FDOPA and 18F-FLT positron emission tomography parametric response maps predict response in recurrent malignant gliomas treated with bevacizumab. Neuro Oncol. 2012; 14(8):1079-89.

Hatakeyama T, Kawai N, Nishiyama Y, et al. 11C-methionine (MET) and 18F-fluorothymidine (FLT) PET in patients with newly diagnosed glioma. European Journal of Nuclear Medicine and Molecular Imaging. 2008; 35(11):2009-2017.

Hayman JA, Callahan JW, Herschtal A, et al. Distribution of proliferating bone marrow in adult cancer patients determined using FLT-PET imaging. International Journal of Radiation Oncology, Biology, Physics. 2010; pp 1-6.

Hiel B, Haanen J, Stokkel M, et al. Vemurafenib plus cobimetinib in unresectable stage IIIc or stage IV melanoma: response monitoring and resistance prediction with positron emission tomography and tumor characteristics (REPOSIT): study protocol of a phase II, open-label, multicenter study. BMC Cancer. 2017; 17(649).

Herrmann K, Buck A, Schuster T, et al. Week one FLT-PET response predicts complete remission to R-CHOP and survival in DLBCL. Oncotarget. 2014; 5(12).

Herrmann K, Eckel F, Schmidt S, et al. In vivo characterization of proliferation for discriminating cancer from pancreatic pseudotumors. Journal of Nuclear Medicine. 2008; 49(9):1437-1444.

Herrmann K, Erkan M, Dobritz M, et al. Comparison of 3'-deoxy-3'-[$^{18}$F]fluorothymidine positron emission tomography (FLT PET) and FDG PET/CT for the detection and characterization of pancreatic tumours. Eur J Nucl Med Mol Imaging. 2012; 39(5):846-51.

Herrmann K, Ott K, Buck AK, et al. Imaging gastric cancer with PET and the radiotracers [18F]-FLT and [18F]-FDG: A comparative analysis. Journal of Nuclear Medicine. 2007; 48(12):1945-1950.

Herrmann K, Wieder HA, Buck AK, et al. Early response assessment using 3'-deoxy-3'-[18F] fluorothymidine positron emission tomography in high-grade non-hodgkin's lymphoma. Clinical Cancer Research. 2007; 13(12):3552-3558.

Hoeben BA, Troost EG, Span PN, et al. 18F-FLT PET during radiotherapy or chemoradiotherapy in head and neck squamous cell carcinoma is an early predictor of outcome. J Nucl Med. 2013; 54(4):532-40.

Hoh C, Burris H, Bendell J, et al. Intermittent dosing of axitinib combined with chemotherapy is supported by 18FLT-PET in gastrointestinal tumours. British Journal of Cancer. 2014; 110: 875-881.

Holdhoff M, Ye X, Supko J, et al. Timed Sequential therapy of the selective T-type calcium channel blocker mibefradil and temozolomide in patients with recurrent high-grade gliomas. Neuro-Oncology. 2017; 19(6): 845-852.

Hong YS, Kim HO, Kim KP, et al. 3'-Deoxy-3'-18F-fluorothymidine PET for the early prediction of response to leucovorin, 5-fluorouracil, and oxaliplatin therapy in patients with metastatic colorectal cancer. J Nucl Med. 2013; 54:1-8.

Honma Y, Terauchi T, Tateishi U, et al. Imaging peritoneal metastasis of gastric cancer with 18F-fluorothymidine positron emission tomography/computed tomography: a proof-of-concept study. British Journal of Radiology. 11 June 2018.

Horn K, Yap J, Agarwal N, et al. FDG and FLT-PET for early measurement of response to 37.5 mg daily sunitinib therapy in metastatic renal cell carcinoma. Cancer Imaging. 2015: 15:15.

Hoshikawa H, Kishino T, Mori T, et al. Comparison of 18F-FLT PET and 18F-FDG PET for detection of cervical lymph node metastases in head and neck cancers. Acta Otolaryngol. 2012; 132(12):1347-54.

Hoshikawa H, Yamamoto Y, Mori T, et al. Predictive value of SUV-based parameters derived from pre-treatment 18F-FLT PET/CT for short-term outcome with head and neck cancers. Ann Nucl Med. 2014; 28: 1020–1026.

Hoshikawa H, Mori T, Kishino T, et al. Changes in 18F-fluorothymidine and 18F-fluorodeoxyglucose positron emission tomography imaging in patients with head and neck cancer treated with chemoradiotherapy. Ann Nucl Med. 2013; 27(4):363-70.

Hoyng L, Frings V, Hoekstra O, et al. Metabolically active tumour volume segmentation from dynamic [18F]FLT PET studies in non-small cell lung cancer. EJNMMI Research. 2015; 5:(26).

Hu J, Yang Z, Gao J, et al. Volumetric Parameters Derived From FLT-PET Performed at Completion of Treatment Predict Efficacy of Carbon-Ion Radiotherapy in Patients with Locally Recurrent Nasopharyngeal Carcinoma. Journal of Cancer. 2020; 11.

ICH Topic Q3C, Impurities: Guideline for Residual Solvents—Tables and List (November 2003 Revision 1).

Idema AJ, Hoffmann AL, Boogaarts HD, et al. 3'-Deoxy-3'-18F-fluorothymidine PET-derived proliferative volume predicts overall survival in high-grade glioma patients. J Nucl Med. 2012; 53(12):1904-10.

Iqbal R, Kramer G, Frings V, et al. Validation of [18F]FLT as a perfusionindependent imaging biomarker of tumour response in EGFR-mutated NSCLC patients undergoing treatment with an EGFR tyrosine kinase inhibitor. EJNMMI Research. 2018; 8:22.

Inubushi M, Saga T, Koizumi M, et al. Predictive value of 3'-deoxy-3'-[18F]fluorothymidine positron emission tomography/computed tomography for outcome of carbon ion radiotherapy in patients with head and neck mucosal malignant melanoma. Ann Nucl Med. 2013; 27(1):1-10.

Jacobs AH, Thomas A, Kracht LW, et al. 18F-fluoro-l-thymidine and 11C-methylmethionine as markers of increased transport and proliferation in brain tumors. Journal of Nuclear Medicine. 2005; 46(12):1948-1958.

Jeong SY, Lim SM. Comparison of 3'-deoxy-3'-[18F]fluorothymidine PET and O-(2-[18F]fluoroethyl)-L-tyrosine PET in patients with newly diagnosed glioma. Nucl Med Biol. 2012; 39(7):977-81.

Johnbeck C, Knigge U, Langer S, et al. Prognostic value of 18F-FLT PET in patients with neuroendocrine neoplasms: A prospective head-to-head comparison with 18F-FDG PET and Ki-67 in 100 patients. J Nucl Med. 2016; 57: 1851–1857.

Joly F, Paciencia M, Bor C, Aide N. Postchemotherapy residual masses in nonseminomatous germ cell tumor patients: 18F FLT PET is unlikely to identify mature teratoma, but imaging of αvβ3 integrin expression could. J Nucl Med. 2011; 52(5):840.

Jung AL, Roan Y, Temple AR. Neonatal death associated with acute transplacental ethanol intoxication, American Journal of Diseases of Children. 1980; 134(4):419-420.

Kahraman D, Holstein A, Scheffler M, et al. Tumor lesion glycolysis and tumor lesion proliferation for response prediction and prognostic differentiation in patients with advanced non-small cell lung cancer treated with erlotinib. Clin Nucl Med. 2012; 37(11):1058-64.

Kairemo K, Santos E, Macapinlac H, et al. Molecular Imaging with 3'-Deoxy-3'-[18F]-Fluorothymidine (18F-FLT) PET/CT for Early Response to Targeted Therapies in Sarcomas: A Pilot Study. Diagnostics. 2020; 10, 125.

Kairemo k, Ravizzini G, Macapinlac H and Subbiah V. An Assessment of early response to targeted therapy via molecular imaging: A pilot study of 30-deoxy-30[(18)F]-Fluorothymidine positron emission tomography 18F-FLT PET/CT in prostate adenocarcinoma. Diagnostics. Epub April 4, 2017.

Kameyama R, Yamamoto Y, Izuishi K, et al. Detection of gastric cancer using 18F-FLT PET: Comparison with 18F-FDG PET. European Journal of Nuclear Medicine and Molecular Imaging. 2009; 36(3):382-388.

Kameyama R, Yamamoto Y, Izuishi K, Sano T, Nishiyama Y. Correlation of 18F-FLT uptake with equilibrative nucleoside transporter-1 and thymidine kinase-1 expressions in gastrointestinal cancer. Nucl Med Commun. 2011; 32(6):460-5.

Kasper B, Egerer G, Gronkowski M, et al. Functional diagnosis of residual lymphomas after radiochemotherapy with positron emission tomography comparing FDG- and FLT-PET. Leukemia & Lymphoma. 2007; 48(4):746-753.

Katlama C, Ghosn J, Tubiana R, et al. MIV-310 reduces HIV viral load in patients failing multiple antiretroviral therapy: results from a 4-week phase II study. AIDS. 2004; 18(9):1299-1304.

Kenny L, Coombes RC, Vigushin DM, et al. Imaging early changes in proliferation at 1 week post chemotherapy: A pilot study in breast cancer patients with 3'-deoxy-3'-[18F]fluorothymidine positron emission tomography. European Journal of Nuclear Medicine and Molecular Imaging. 2007; 34(9):1339-1347.

Kenny LM, Vigushin DM, Al-Nahhas A, et al. Quantification of cellular proliferation in tumor and normal tissues of patients with breast cancer by [18F]fluorothymidine-positron emission tomography imaging: Evaluation of analytical methods. Cancer Research. 2005; 65(21):10104-10112.

Kim J, Chae S, Kim J, et al. 3'-Deoxy-3'-18F-Fluorothymidine and 18F-Fluorodeoxyglucose positron emission tomography for the early prediction of response to Regorafenib in patients with metastatic colorectal cancer refractory to all standard therapies. European Journal of Nuclear Medicine and Molecular Imaging. 2019; 46:1713–1722.

Kishino T, Hoshikawa H, Nishiyama Y, Yamamoto Y, Mori N. Usefulness of 3'-deoxy-3'-18F-fluorothymidine PET for predicting early response to chemoradiotherapy in head and neck cancer. J Nucl Med. 2012; 53(10):1521-7.

Kobe C, Scheffler M, Holstein A, et al. Predictive value of early and late residual 18F-fluorodeoxyglucose and 18F-fluorothymidine uptake using different SUV measurements in patients with non-small-cell lung cancer treated with erlotinib. Eur J Nucl Med Mol Imaging. 2012; 39(7):1117-27.

Koizumi M, Saga T, Inubushi M, et al. Uptake decrease of proliferative PET tracer 18FLT in bone marrow after carbon ion therapy in lung cancer. Molecular Imaging and Biology, 2010.

Kong XB, Zhu QY, Vidal PM, et al. Comparisons of anti-human immunodeficiency virus activities, cellular transport, and plasma intracellular pharmacokinetics of 3'-fluoro-3'-deoxythymidine and 3'-azido-3'-deoxythymidine. Antimicrobial Agents and Chemotherapy. 1992; 36(4):808-818.

Kostakoglu L, Duan F, Idowu M, et al. A Phase II study of 39-Deoxy-39-18F-Fluorothymidine PET in the assessment of early response of breast cancer to neoadjuvant chemotherapy: Results from ACRIN 6688. J Nucl Med. 2015; 56: 1681–1689.

Kudomi N, Maeda2 Y, Hatakeyama3 T, Yamamoto4 Y, Nishiyama Y. Fully parametric imaging with reversible tracer 18F-FLT within a reasonable time. Radiol Phys Technol. Epub July 5, 2016.

Kupiecki FP, Coon MJ. Methylmalonic semialdehyde. Preparative Biochemistry. 1960; 7:69-71.

Langen P, Etzold G, Hintsche R, Kowollik G. 3'-Deoxy-3'-fluorothymidine, a new selective inhibitor of DNA synthesis. Acta Biologica et Medica Germanica. 1969; 23(6):759-766.

Langen P, Graetz H. Cell death resulting from inhibition by 3'-deoxy-3'-fluorothymidine, cytosine-arabinoside, 5-fluoro-2'-deoxyuridine, and hydroxyurea of DNA synthesis in cultured Ehrich ascites carcinoma cells. Studia Biophys. 1972; 31/32:359-366.

Langen P, Kowollok G, Etzold G, Venner H, Reinhert H. The phosphorylation of 3'-deoxy-3'-fluorothymidine and its incorporation into DNA in a cell free system from tumor cells. Acta Biologica et Medica Germanica. 1972; 29(4):483-494.

Larsson A, Johansson A, Axelsson J, et al. Evaluation of an attenuation correction method for PET/MR imaging of the head based on substitute CT images. MAGMA. 2013; 26(1):127-36.

Laymon CM, Oborski MJ, Lee VK, et al. Combined imaging biomarkers for therapy evaluation in glioblastoma multiforme: correlating sodium MRI and F-18 FLT PET on a voxel-wise basis. Magn Reson Imaging. 2012; 30(9):1268-78.

Lee H, Kim S, Kim Y, et al. Early determination of prognosis by interim 39-Deoxy-39-18FFluorothymidine PET in patients with non-hodgkin lymphoma. J Nucl Med. 2014; 55: 216–222.

Leimgruber A, Möller A, Everitt S, et al. Effect of platinum-based chemoradiotherapy on cellular proliferation in bone marrow and spleen, estimated by 18FFLT PET/CT in patients with locally advanced non–small cell lung cancer. J Nucl Med. 2014; 55: 1075–1080.

Leonard JP, LaCasce AS, Smith MR, et al. Selective CDK4/6 inhibition with tumor responses by PD0332991 in patients with mantle cell lymphoma. Blood. 2012; 119(20):4597-607.

Lin W, Dai S, Chen T, et al. Expression of 58-kD microspherule protein (MSP58) is highly correlated with pet imaging of tumor malignancy and cell proliferation in glioma patients. Cell Physiol Biochem. 2016; 38: 635-645.

Liu J, Li C, Hu M, et al. Exploring spatial overlap of high-uptake regions derived from dual tracer positron emission tomography–computer tomography imaging using 18F-Fluorodeoxyglucose and 18F-Fluorodeoxythymidine in nonsmall cell lung cancer patients. A prospective pilot study. Medicine. May 2015; 94(17).

Liu D, Chalkidou A, Landau D, Marsden P, and Fenwick J. 18F-FLT uptake kinetics in head and neck squamous cell carcinoma: A PET imaging study. Medical Physics. April 2014; 41(4).

Liu CJ, Wang J, Kuo WH, Yen RF. High 18F-fluorothymidine uptake for invasive thymoma. Clin Nucl Med. 2012; 37(10):991-2.

Lodge M, Holdhoff M, Leal J, et al. Repeatability of 18F-FLT pet in a multi-center study of patients with high grade glioma. J Nucl Med. Epub September 29, 2016.

Lovinfosse P, Rousseau C, Pierga J, et al. Dual Time Point [18F]FLT-PET for Differentiating Proliferating Tissues vs Nonproliferating Tissues. EJNMMI Research. 2019; 9:109.

Lu L, Samuelsson L, Bergstrom M, et al. Rat studies comparing 11C-FMAU, 18F-FLT, and 76Br-BFU as proliferation markers. Journal of Nuclear Medicine. 2002; 43(12):1688-1698.

Lubberink M, Direcks W, Emmering J, et al. Validity of simplified 3'-deoxy-3'-[18F]fluorothymidine uptake measures for monitoring response to chemotherapy in locally advanced breast cancer. Mol Imaging Biol. 2012; 14(6):777-82.

Lundgren B, Bottiger D, Ljungdahl-Stahle. Antiviral effects of 3'-fluorothymidine and 3'-azidothymidine in cynomolgus monkeys infected with simian immunodeficiency virus. Journal of Acquired Immune Deficiency Syndromes. 1991; 4(5):489-498.

Ma C, Li D, Yin Y, and Cao J. Comparison of characteristics of 18F-fluorodeoxyglucose and 18F-fluorothymidine PET during staging of esophageal squamous cell carcinoma. Nuclear Medicine Communications. 2015; 36:1181–1186.

Ma D, Galanis E, Anderson S, et al. A phase II trial of everolimus, temozolomide, and radiotherapy in patients with newly diagnosed glioblastoma: NCCTG N057K. Neuro-Oncology. 2015; 17(9): 1261–1269.

Machulla HJ. Procedure for routine synthesis of [18F]FLT in high activities. Journal of Nuclear Medicine. 2001; 42(5):257P.

Malkowski B, Staniuk T, Urutek E, et al. 18F-FLT PET/CT in patients with gastric carcinoma. Hindawi. 2013.

Marti-Climent J, Dominguez-Prado I, Garcia-Velloso M, et al. [18F]Fluorothymidine-positron emission tomography in patients with locally advanced breast cancer under bevacizumab

treatment: Usefulness of different quantitative methods of tumor proliferation. Rev Esp Med Nucl Imagen Mol. 2014; 33(5): 280-285.

Matthes E, Lehmann C, Scholz D, et al. Inhibition of HIV-associated reverse transcriptase by sugar-modified derivatives of thymidine 5'-triphosphate in comparison to cellular DNA polymerases α and β. Biochemical and Biophysical Research Communications. 1987; 148(1):78-85.

Matthes E, Lehmann C, Scholz D, Rosenthal HA, Langen P. Phosphorylation, anti-HIV activity and cytotoxicity of 3'-fluorothymidine. Biochemical and Biophysical Research Communications. 1988; 153(2):825-831.

Mattsson S. Johansson L. Leide Svegborn S. Liniecki J. Nosske D. Riklund KA. et al. Radiation dose to patients from radiopharmaceuticals: A compendium of current information related to frequently used substances. (ICRP Publication 128) Ann ICRP2015; 44:7–321.

McGuire S, Bhatai S, Sun W, et al. Using [18F]Fluorothymidine imaged with positron emission tomography to quantify and reduce hematologic toxicity due to chemoradiation therapy for pelvic cancer patients. Int J Radiat Oncol Biol Phys. April 11, 2016; 96(1).

McGuire SM, Menda Y, Boles Ponto LL, Gross B, Buatti J, Bayouth JE. 3'-deoxy-3'-[$^{18}$F]fluorothymidine PET quantification of bone marrow response to radiation dose. Int J Radiat Oncol Biol Phys. 2011; 81(3):888-93.

McGuire SM, Menda Y, Ponto LL, Gross B, Juweid M, Bayouth JE. A methodology for incorporating functional bone marrow sparing in IMRT planning for pelvic radiation therapy. Radiother Oncol. 2011; 99(1):49-54.

McHugh C, Lawhorn-Crews j, Modi D, et al. Effects of capecitabine treatment on the uptake of thymidine analogs using exploratory PET imaging agents: 18F-FAU, 18F-FMAU, and 18F-FLT. Cancer Imaging. 2016; 16(34).

McKinley E, Watchmaker J, Chakravarthy A, et al. [18F]-FLT PET to predict early response to neoadjuvant therapy in KRAS wild-type rectal cancer: a pilot study. Ann Nucl Med. 2015; 29:535–542.

McKinley ET, Smith RA, Tanksley JP, et al. [18F]FLT-PET to predict pharmacodynamic and clinical response to cetuximab therapy in Ménétrier's disease. Ann Nucl Med. 2012; 26(9):757-63.

Mendes B, Ferreira A, Nascimento T, Et Al. New Radiation Dosimetry Estimates For [18f]Flt Based on Voxelized Phantoms. Radiat Res. 2018; 190(1): 37-44.

Mena E, Lindenberg M, Turkbey B, et al. A pilot study of the value of 18F-Fluoro-Deoxy-Thymidine PET/CT in predicting viable lymphoma in residual 18F-FDG avid masses after completion of therapy. Clin Nucl Med. 2014; 39: 874Y881.

Minamimoto R, Fayad L, Advani R, et al. Diffuse large b-cell lymphoma: prospective multicenter comparison of early interim FLT PET/CT versus FDG PET/CT with IHP, EORTC, deauville, and percist criteria for early therapeutic monitoring. Radiology. July 2016; 280(1).

Mileshkin L, Hicks RJ, Hughes BG, et al. Changes in 18F-fluorodeoxyglucose and 18F-fluorodeoxythymidine positron emission tomography imaging in patients with non–small cell lung cancer treated with erlotinib. Clin Cancer Res. 2011; 17(10):3304-15.

Mitamura K, Yamamoto Y, Kudomi N, et al. Intratumoral heterogeneity of 18F-FLT uptake predicts proliferation and survival in patients with newly diagnosed gliomas. Ann Nucl Med. Epub September 29, 2016.

Mock BH, Winkle W, Vavrek MT. Technical note: A color spot test for the detection of kryptofix® [2.2.2] in [18F]FDG preparations. Nuclear Medicine & Biology. 1997; 24(2):193-195.

Mogensen M, Loft A, Aznar M, et al. FLT-PET for early response evaluation of colorectal cancer patients with liver metastases: a prospective study. EJNMMI Research. 2017; 7(56).

Muijs CT, Beukema JC, Widder J, et al. 18F-FLT-PET for detection of rectal cancer. Radiother Oncol. 2011; 98(3):357-9.

Muzi M, Spence AM, O'Sullivan F, et al. Kinetic analysis of 3' – deoxy-3' – 18F- fluorothymidine in patients with gliomas. Journal of Nuclear Medicine. 2006; 47(10):1612-1621.

Muzi M, Vesselle H, Grierson JR, et al. Kinetic analysis of 3'-deoxy-3'-fluorothymidine PET studies: Validation studies in patients with lung cancer. Journal of Nuclear Medicine. 2005; 46(2):274-282.

Nakajo M, Kajiya Y, Tani A, et al. A pilot study for texture analysis of 18F-FDG and 18F-FLT-PET/CT to predict tumor recurrence of patients with colorectal cancer who received surgery. Eur J Nucl Med Mol Imaging. 2017; 44: 2158–2168.

Nakajo M, Kajiya Y, Tani A, et al. A pilot study of the diagnostic and prognostic values of FLT-PET/CT for pancreatic cancer: comparison with FDG-PET/CT. Abdom Radiol. Epub November 28, 2016.

Nakajo M, Jinguji M, Fukukura Y, et al. FDG-PET/CT and FLT-PET/CT for differentiating between lipid-poor benign and malignant adrenal tumours. Eur Radiol. 2015; 25:3696–3705.

Nakajo M, Nakajo M, Kajiya Y, et al. Correlations of 18F-fluorothymidine uptake with pathological tumour size, Ki-67 and thymidine kinase 1 expressions in primary and metastatic lymph node colorectal cancer foci. Eur Radiol. 2014; 24: 3199–3209.

Nakajo M, Nakajo M, Jinguji M, et al. Diagnosis of metastases from postoperative differentiated thyroid cancer: comparison between FDG and FLT PET/CT studies. Radiology. 2013; 267(3):891-901.

Nakajo M, Nakajo M, Kajiya Y, et al. Diagnostic performance of 18F-fluorothymidine PET/CT for primary colorectal cancer and its lymph node metastasis: comparison with 18F-fluorodeoxyglucose PET/CT. Eur J Nucl Med Mol Imaging. 2013; 37:607-608.

Nakajo M, Nakajo M, Kajiya Y, et al. High FDG and low FLT uptake in a thyroid papillary carcinoma incidentally discovered by FDG PET/CT. Clin Nucl Med. 2012; 37(6):607-8.

Nikaki A, Papadopoulos V, Valotassiou V, et al. Evaluation of the Performance of 18F-Fluorothymidine Positron Emission Tomography/Computed Tomography (18F-FLT-PET/CT) in Metastatic Brain Lesions. Diagnostics. 26 January 2019

Norikane T, Yamamoto Y, Maeda Y, et al. Comparative evaluation of 18F-FLT and 18FFDG for detecting cardiac and extra-cardiac thoracic involvement in patients with newly diagnosed sarcoidosis. EJNMMI Research. 2017; 7(69).

Nowosielski M, DiFranco M, Putzer D, et al. An intra-individual comparison of MRI, [18F]-FET and [18F]-FLT PET in patients with high-grade gliomas. PLOS ONE. 2014; 9(4): e95830.

Nyflot M, Kruser T, Trynor A, et al. Phase 1 trial of bevacizumab with concurrent chemoradiation therapy for squamous cell carcinoma of the head and neck with exploratory functional imaging of tumor hypoxia, proliferation, and perfusion. Int J Radiation Oncol Biol Phys. 2015; 91(5): pp. 942e951.

Nyflot MJ, Harari PM, Yip S, Perlman SB, Jeraj R. Correlation of PET images of metabolism, proliferation and hypoxia to characterize tumor phenotype in patients with cancer of the oropharynx. Radiother Oncol. 2012; 105(1):36-40.

Okada M, Hatakeyama T, Ogawa D, et al. Increased diagnostic yield obtained by MRI/PET fusion image for recurrent glioma: Usefulness of 3'-deoxy-3'-[18F]fluorothymidine(FLT). Abstracts for the Eighth Congress of the European Association for Neuro-Oncology (EANO): September 12-14, 2008 Barcelona, Spain. Neuro-Oncology. 2008; 10(1):1126.

Ogawa T, Kawai N, Miyake K, et al. Diagnostic Value of PET/CT with 11Cmethionine (MET) and 18F-Fluorothymidine (FLT) in Newly Diagnosed Glioma Based on the 2016 WHO classification. EJNMMI Research. 2020; 10:44.

O'Sullivan C, Lindenberg M, Bryla C, et al. ANG1005 for breast cancer brain metastases: Correlation between 18F-FLT–PET after first cycle and MRI in response assessment. Breast Cancer Res Treat. 2016; 160: 51–59.

Ott K, Herrmann K, Schuster T, et al. Molecular imaging of proliferation and glucose utilization: utility for monitoring response and prognosis after neoadjuvant therapy in locally advanced gastric cancer. Ann Surg Oncol. 2011; 18(12):3316-23.

Palmieri C, Szydlo R, Miller M, et al. IPET study: an FLT-PET window study to assess the activity of the steroid sulfatase inhibitor irosustat in early breast cancer. Breast Cancer Res Treat (2017) 166:527–539.

Pantaleo MA, Landuzzi L, Nicoletti G, et al. Advances in preclinical therapeutics development using small animal imaging and molecular analyses: The gastrointestinal stromal tumors model. Clinical and Experimental Medicine. 2009; 9(3):199-205.

Pfannenberg C, Aschoff P, Dittmann H, et al. PET/CT with 18F-FLT: Does it improve the therapeutic management of metastatic germ cell tumors? Journal of Nuclear Medicine. 2010; 51(6):845–853.

Pio BS, Park CK, Pietras R, et al. Usefulness of 3'-[F-18]fluoro-3'-deoxythymidine with positron emission tomography in predicting breast cancer response to therapy. Molecular Imaging and Biology. 2006; 8(1):36-42.

Pretz J, Blake M, Killoran J, et al. Pilot study on the impact of F18-labeled thymidine PET/CT on gross tumor volume identification and definition for pancreatic cancer. Practical Radiation Oncology. 2017.

Price SJ, Fryer TD, Cleij MC, et al. Imaging regional variation of cellular proliferation in gliomas using 3'-deoxy-3'-[18F]fluorothymidine positron-emission tomography: An image-guided biopsy study. Clinical Radiology. 2009; 64:52-63.

Qi S, Zhongyi Y, Yingjia Z, and Chaosu H. 18F-FLT and 18F-FDG PET/CT in predicting response to chemoradiotherapy in nasopharyngeal carcinoma: Preliminary Results. Epub January 16, 2017.

Quon A, Chang ST, Chin F, et al. Initial evaluation of [18F]-fluorothymidine (FLT) PET/CT scanning for primary pancreatic cancer. European Journal of Nuclear Medicine and Molecular Imaging. 2008; 35(3):527-531.

Rasey JS, Grierson JR, Wiens LW, Kolb PD, Schwartz JL. Validation of FLT uptake as a measure of thymidine kinase-1 activity in A549 carcinoma cells. Journal of Nuclear Medicine. 2002; 43(9):1210-1217.

Rayamajhi S, Mittal B, Maturu V, et al. 18F-FDG and 18F-FLT PET/CT imaging in the characterization of mediastinal lymph nodes. Ann Nucl Med. 2016; 30: 207–216.

Rendl G, Rettenbacher L, Holzmannhofer J, et al. Assessment of response to neoadjuvant radiochemotherapy with F-18 FLT and F-18 FDG PET/CT in patients with rectal cancer. Ann Nucl Med. 2015; 29:284–294.

Ribas A, Benz MR, Allen-Auerbach MS, et al. Imaging of CTLA4 blockade-induced cell replication with 18F-FLT PET in patients with advanced melanoma treated with tremelimumab. Journal of Nuclear Medicine. 2010; 51(3):340-346.

Richard SD, Bencherif B, Edwards RP, et al. Noninvasive assessment of cell proliferation in ovarian cancer using [18F] 3'deoxy-3-fluorothymidine positron emission tomography/computed tomography imaging. Nucl Med Biol. 2011; 38(4):485-91.

Roels S, Slagmolen P, Nuyts J, et al. Biological image-guided radiotherapy in rectal cancer: Is there a role for FMISO or FLT, next to FDG? Acta Oncologica. 2008; 47(7):1237-1248.

Sachpekidis C, Goldschmidt H, Kopp-Schneider A, Dimitrakopoulou-Strauss A. Assessment of glucose metabolism and cellular proliferation in multiple myeloma: a first report on combined 18F-FDG and 18F-FLT PET/CT imaging. EJNMMI Research (2018) 8:28.

Saga T, Kawashima H, Araki N, et al. Evaluation of primary brain tumors with FLT-PET: Usefulness and limitations. Clinical Nuclear Medicine. 2006; 31:774-780.

Saga T, Koizumi M, Inubushi M, et al. PET/CT with 3'-deoxy-3'-[18F]fluorothymidine for lung cancer patients receiving carbon-ion radiotherapy. Nucl Med Commun. 2011; 32(5):348-55.

Scarpelli M, Zahm C, Perlman S, et al. FLT PET/CT imaging of metastatic prostate cancer patients treated with pTVG-HP DNA vaccine and pembrolizumab. Journal for Immuno Therapy of Cancer. 2019; 7:23.

Scarpelli M, Rampurwala M, Eickhoff J, et al. Pharmacodynamic study using FLT PET/CT in advanced solid malignancies treated with a sequential combination of X-82 and docetaxel. Cancer Chemotherapy and Pharmacology. 2018; 82:211–219.

Scheffler M, Kobe C, Zander T, et al. Monitoring reversible and irreversible EGFR inhibition with erlotinib and afatinib in a patient with EGFR-mutated non-small cell lung cancer (NSCLC) using sequential [18F]fluorothymidine (FLT-)PET. Lung Cancer. 2012; 77(3):617-20.

Scheffler M, Zander T, Nogova L, et al. Prognostic impact of [18F]fluorothymidine and [18F]fluoro-D-glucose baseline uptakes in patients with lung cancer treated first-line with erlotinib. PLoS One. 2013; 8(1):e53081.

Schiepers C, Chen W, Dahlbom M, et al. [18F]-fluorothymidine kinetics of malignant brain tumors. European Journal of Nuclear Medicine and Molecular Imaging. 2007; 34(7):1003-1011.

Schöder H, Zelenetz A, Hamlin P, et al. Prospective study of 39-Deoxy-39-18F-Fluorothymidine PET for early interim response assessment in advanced-stage B-Cell Lymphoma. J Nucl Med. 2016; 57: 728–734.

Schöder H, Zelenetz A, Hamlin P, et al. Prospective study of flt pet for early interim response assessment in advanced stage b-cell lymphoma. J Nucl Med. December 30, 2015.

Sharma R, Mapelli P, Hanna G, et al.Evaluation of 18F-fluorothymidine positron emission tomography ([18F]FLT-PET/CT) methodology in assessing early response to chemotherapy in patients with gastrooesophageal cancer. EJNMMI Research. 2016; 6(81).

Shaw G, Warrener RN. Purines, pyrimidines, and glyoxalines. PartVII. New syntheses of 2-thiouracils and 2-thiothymines. Journal of the Chemical Society. 1958; 153-156.

Shields AF, Briston DA, Chandupatla S, et al. A simplified analysis of [18F]3'-deoxy-3'-fluorothymidine metabolism and retention. European Journal of Nuclear Medicine and Molecular Imaging. 2005; 32(11):1269-1275.

Shields AF, Grierson JR, Dohmen BM, et al. Imaging proliferation in vivo with [F-18]FLT and positron emission tomography. Nature Medicine. 1998; 4(11):1334-1336.

Shields AF, Lawhorn-Crews JM, Briston DA, et al. Analysis and reproducibility of 3'-deoxy-3' –[18F] fluorothymidine positron emission tomography imaging in patients with non-small cell lung cancer. Clinical Cancer Research. 2008; 14(14):4463-4468.

Shinomiya A, Miyake K, Okada M, et al. ( 3'-Deoxy-3'-[18F]-fluorothymidine [18F]-FLT transport in newly diagnosed glioma: correlation with nucleoside transporter expression, vascularization, and blood-brain barrier permeability. Brain Tumor Pathol, 2013.

Shinomiya A, Kawai N, Okada M, et al. Evaluation of 3'-deoxy-3'-[18F]-fluorothymidine (18F-FLT) kinetics correlated with thymidine kinase-1 expression and cell proliferation in newly diagnosed gliomas. Eur J Nucl Med Mol Imaging. 2013; 40(2):175-85.

Smyczek-Gargya B, Fersis N, Dittmann H, et al. PET with [18F]fluorothymidine for imaging of primary breast cancer: a pilot study. European Journal of Nuclear Medicine and Molecular Imaging. 2004; 31(5):720–724.

Sohn HJ, Yang YJ, Ryu JS, et al. [18F] fluorothymidine positron emission tomography before and 7 days after gefitinib treatment predicts response in patients with advanced adenocarcinoma of the lung. Clinical Cancer Research. 2008; 14(22):7423-7429.

Spence AM, Muzi M, Link JM, et al. NCI-sponsored trial for the evaluation of safety and preliminary efficacy of FLT as a marker of proliferation in patients with recurrent gliomas: Safety studies. Molecular Imaging and Biology. 2008; 10:271-280.

Staniuk T, Małkowski B, Srutek E, et al. Comparison of FLT-PET/CT and CECT in gastric.cancer diagnosis. Abdom Radiol. 2016; 41: 1349–1356.

Staniuk T, Zegarski W, Małkowski B, Jankowski M, Klag M, Pietrzak T. Evaluation of FLT-PET/CT usefulness in diagnosis and qualification for surgical treatment of gastric cancer. Contemp Oncol (Pozn). 2013; 17(2):165-70.

Sundseth R, Joyner SS, Moore JT, Dornsife RE, Dev, IK. The anti-human immunodeficiency virus agent 3'-fluorothymidine induces DNA damage and apoptosis in human lymphoblastiod cells. Antimicrobial Agents and Chemotherapy. 1996; 40(2):331-335.

Thureau S, Chaumet-Riffaud P, Modzelewski R, et al. Interobserver agreement of qualitative analysis and tumor delineation of 18F-fluoromisonidazole and 3-deoxy-3-18F-fluorothymidine PET images in lung cancer. J Nucl Med. 2013; 54:1543–1550.

Tian J, Yang X, Yu L, et al. A multicenter clinical trial on the diagnostic value of dual-tracer PET/CT in pulmonary lesions using 3'-deoxy-3'-[18F]-fluorothymidine and [18F]-FDG. Journal of Nuclear Medicine. 2008; 49(2):186-194.

Trigonis I, Koh K, Taylor B, et al. Early reduction in tumour [18F]fluorothymidine (FLT) uptake in patients with non-small cell lung cancer (NSCLC) treated with radiotherapy alone. Eur J Nucl Med Mol Imaging. 2014; 41: 682–693.

Tripathi M, Sharma R, D'Souza M, et al. Comparative evaluation of F-18 FDOPA, F-18 FDG, and F-18 FLT-PET/CT for metabolic imaging of low grade gliomas. Clinical Nuclear Medicine. 2009; 34(12):878-883.

Troost EGC, Bussink J, Hoffmann AL, et al. 18F-FLT PET/CT for early response monitoring and dose escalation in oropharngeal tumors. Journal of Nuclear Medicine. 2010; 51:866-874.

Troost EGC, Vogel WV, Merkx MAW, et al. 18F-FLT PET does not discriminate between reactive and metastatic lymph nodes in primary head and neck cancer patients. Journal of Nuclear Medicine. 2007; 48(5):726-735.

Tsujikawa T, Tasaki T, Hosono N, et al. 18F-FLT PET/MRI for bone marrow failure syndrome-initial experience. EJNMMI Research. 2019; 9:16.

Turcotte E, Wiens LW, Grierson JR, Peterson LM, Wener MH, Vesselle H. Toxicology evaluation of radiotracer doses of 3'-deoxy-3'-[18F]Fluorothymidine (18F-FLT) for human PET Imaging:

Laboratory analysis of serial blood samples and comparison to previously investigated therapeutic FLT doses. BMC Nuclear Medicine. 2007; 7(3).

Ueberroth B, Lawhorn-Crews, J, Heilbrun L, et al. The use of 3'-Deoxy-3'-18F-Fluorothymidine (FLT) PET in The Assessment of Long-Term Survival in Breast Cancer Patients Treated with Neoadjuvant Chemotherapy. Ann Nucl Med. 2019 June; 33(6): 383–393.

Ullrich R, Backes H, Li H, et al. Glioma proliferation as assessed by 3'-fluoro-3'-deoxy-L-thymidine positron emission tomography in patients with newly diagnosed high-grade glioma. Clinical Cancer Research. 2008; 14(7):2049-2055.

Umeda Y, Tsujikawa T, Anzai M, et al. The Vertebral 3'-Deoxy-3'-18F-Fluorothymidine Uptake Predicts the Hematological Toxicity After Systemic Chemotherapy in Patients with Lung Cancer. European Radiology. 2019; 29:3908–3917.

Van Westreenen HL, Cobben DCP, Jager PL, et al. Comparison of 18F-FLT PET and 18F-FDG PET in esophageal cancer. Journal of Nuclear Medicine. 2005; 46(3):400-404.

Vanderhoek M, Juckett MB, Perlman SB, Nickles RJ, Jeraj J. Early assessment of treatment response in patients with AML using [18F]FLT PET imaging. Leukemia Research. 2011; 35(3):310-316.

Vanderhoek M, Perlman SB, Jeraj R. Impact of different standardized uptake value measures on PET-based quantification of treatment response. J Nucl Med, 2013.

Vercellino L, Ouvrier M, Barre, et al. Assessing bone marrow activity in patients with myelofibrosis: Results of a pilot study of 18F-FLT PET. J Nucl Med 2017; 58:1603–1608.

Veronese M, Rizzo G, Aboagye E, Bertoldo A. Parametric imaging of 18F-fluoro-3-deoxy-3-L-fluorothymidine PET data to investigate tumour heterogeneity. Eur J Nucl Med Mol Imaging. 2014; 41: 1781–1792.

Vesselle H, Grierson J, Muzi M, et alE. In vivo validation of 3'deoxy-3'-[18F]fluorothymidine ([18F]FLT) as a proliferation imaging tracer in humans: Correlation of [18F]FLT uptake by positron emission tomography with Ki-67 immunohistochemistry and flow cytometry in human lung tumors. Clinical Cancer Research. 2002; 8(11):3315-3323.

Vesselle H, Grierson J, Peterson LM, Muzi M, Mankoff DA, Krohn KA. 18F-Fluorothymidine radiation dosimetry in human PET imaging studies. Journal of Nuclear Medicine. 2003; 44(9):1482–1488.

Visvikis D, Francis D, Mulligan R, et al. Comparison of methodologies for the in vivo assessment of 18FLT utilisation in colorectal cancer. European Journal of Nuclear Medicine and Molecular Imaging. 2004; 31(2):169-178.

Vojtisek R, Ferda J, Finek J, et al. Effectiveness of PET/CT with 18F-fluorothymidine in the staging of patients with squamous cell head and neck carcinomas before radiotherapy. Reports of Prac Oncol Radiother. 2015; 20: 210-216.

Wagner M, Seitz U, Buck A, et al. 3'-[18F]fluoro-3'-deoxythymidine [18F]-FLT as positron emission tomography tracer for imaging proliferation in a murine b-cell lymphoma model and in the human disease. Cancer Research. 2003; 63(10):2681-2687.

Wang R, Xu B, Liu C, et al. Prognostic value of interim fluorodeoxyglucose and fluorothymidine PET/CT in diffuse large B-cell lymphoma. British Journal of Radiology. 09 July 2018.

Wang X, He Y, Zhou W, et al. Mismatched intratumoral distribution of [18F] fluorodeoxyglucose and 3'-deoxy-3'-[18F] fluorothymidine in patients with lung cancer. Oncology Letters. 2017; 14: 5279-5284.

Wang J, Kuo W, Shih T, and Yen R. Using 18F-FLT PET to distinguish between malignant and benign breast lesions with suspicious findings in mammography and breast ultrasound. Ann Nucl Med. 2014; 28: 941–949.

Wang C, Guo W, Zhou M, et al. The Predictive and prognostic value of early metabolic response assessed by positron emission tomography in advanced gastric cancer treated with chemotherapy. Clinical Cancer Research. November 25, 2015.

Wang R, Zhu H, Chen Y, et al. Standardized uptake value based evaluation of lymphoma by FDG and FLT PET/CT. Hematol Oncol, 2013.

Wesolowski R, Stover D, Lustberg M, et al. Phase I Study of Veliparib on an Intermittent and Continuous Schedule in Combination with Carboplatin in Metastatic Breast Cancer: A Safety and [18F]-Fluorothymidine Positron Emission Tomography Biomarker Study. The Oncologist. 2020; 25: 1158–1169.

Wieder H, Beer A, Siveke J, et al. 18F-Fluorothymidine PET for predicting survival in patients with resectable pancreatic cancer. Oncotarget. 2018; 9(11).

Wieder HA, Geinitz H, Rosenberg R, et al. PET imaging with [18F]3'-deoxy-3'-fluorothymidine for predication of response to neoadjuvant treatment in patients with rectal cancer. European Journal of Nuclear Medicine and Molecular Imaging. 2007; 34(6):878-883.

Willaime JM, Turkheimer FE, Kenny LM, Aboagye EO. Quantification of intra-tumour cell proliferation heterogeneity using imaging descriptors of 18F fluorothymidine-positron emission tomography. Phys Med Biol. 2013; 58(2):187-203.

Williams K, Holter-Chakrabarty J, Lindenberg L, et al. Imaging of subclinical haemopoiesis after stem-cell transplantation in patients with haematological malignancies: a prospective pilot study. Lancet Haematol. 2018; 5: e44–52.

Wobus AM. Clastogenic activity of cytosine arabinoside and 3'-deoxy-3'-fluorothymidine in Ehrlich ascites tumor cells in vitro. Mutation Research/Genetic Toxicology. 1976; 40(2):101-105.

Wondergem M, Rizvi S, Jauw Y, et al. 18F-FDG or 39-Deoxy-39-18F-Fluorothymidine to detect transformation of follicular lymphoma. J Nucl Med. 2015; 56: 216–221.

Wondergem M, Herrmann K, Syrbu S, et al. 18 F-fluorothymidine uptake in follicular lymphoma and error-prone DNA repair. EJNMMI Research. 2014; 4:3.

Woolf D, Beresford M, Li P, et al. Evaluation of FLT-PET-CT as an imaging biomarker of proliferation in primary breast cancer. British Journal of Cancer. 2014; 110, 2847-2854.

Wyss J, Carmona R, Karunamuni R, et al. [18F]Fluoro-2-deoxy-2-D-glucose versus 30-deoxy-30-[18F] fluorothymidine for defining hematopoietically active pelvic bone marrow in gynecologic patients. Radiother Oncol. 2016; 118: 72-78.

Xu B, Guan Z, Liu C, et al. Can multimodality imaging using 18F-FDG/18F-FLT PET/CT benefit the diagnosis and management of patients with pulmonary lesions? European Journal of Nuclear Medicine and Molecular Imaging. 2010; 38(2):285-292.

Xu BX, Liu CB, Wang RM, et al. The influence of interpreters' professional background and experience on the interpretation of multimodality imaging of pulmonary lesions using 18F-3'-deoxy-fluorothymidine and 18F-fluorodeoxyglucose PET/CT. PLoS One. 2013; 8(4):e60104.

Yamamoto Y, Nishiyama Y, Ishikawa S, et al. 3'-Deoxy-3'-18F-fluorothymidine as a proliferation imaging tracer for diagnosis of lung tumors: Comparison with 2-deoxy-2-18F-fluoro-d-glucose. Journal of Computer Assisted Tomography. 2008; 32(3):432-437.

Yamamoto Y, Nishiyama Y, Ishikawa S, et al. Correlation of 18F-FLT and 18F-FDG uptake on PET with Ki-67 immunohistochemistry in non-small cell lung cancer. European Journal of Nuclear Medicine and Molecular Imaging. 2007; 34(10):1610-1616.

Yamamoto Y, Nishiyama Y, Kimura N, et al. Comparison of 18F-FLT PET and 18F-FDG PET for preoperative staging in non-small cell lung cancer. European Journal of Nuclear Medicine and Molecular Imaging. 2008; 35(2):236-245.

Yamamoto Y, Ono Y, Aga F, Kawai N, Kudomi N, Nishiyama Y. Correlation of 18F-FLT uptake with tumor grade and Ki-67 immunohistochemistry in patients with newly diagnosed and recurrent gliomas. J Nucl Med. 2012; 53(12):1911-5.

Yamamoto Y, Wong TZ, Turkington TG, Hawk TC, Reardon DA, Coleman RE. 3'-Deoxy-3'-[F-18]fluorothymidine positron emission tomography in patients with recurrent glioblastoma multiforme: Comparison with Gd-DTPA enhanced magnetic resonance imaging. Molecular Imaging and Biology. 2006; 8:340-347.

Yamane T, Takaoka A, Kita M, Imai Y, Senda M. 18F-FLT PET performs better than 18F-FDG PET in differentiating malignant uterine corpus tumors from benign leiomyoma. Ann Nucl Med. 2012; 26(6):478-84.

Yang W, Zhang Y, Fu Z, et al. Imaging proliferation of 18F-FLT PET/CT correlated with the expression of microvessel density of tumour tissue in non-small-cell lung cancer. Eur J Nucl Med Mol Imaging. 2012; 39:1289–1296.

Yang W, Zhang Y, Fu Z, et al. Imaging of proliferation with 18F-FLT PET/CT versus 18F-FDG PET/CT in non-small-cell lung cancer. European Journal of Nuclear Medicine and Molecular Imaging. 2010; 37(7):1291-1299.

Yap CS, Czernin J, Fishbein MC, et al. Evaluation of thoracic tumors with 18F-fluorothymidine and 18F-fluorodeoxyglucose-positron emission tomography. Chest. 2006; 129(2):393-401.

Ye Y, Calcagno C, Binderup T, et al. Imaging macrophage and hematopoietic progenitor proliferation in atherosclerosis. Circulation Research. October 23, 2015.

Yeh R, Trager M, Rizk E, et al. FLT-PET At 6 Weeks Predicts Response Assessed by CT at 12 Weeks in Melanoma Patients Treated with Pembrolizumab. Clinical Nuclear Medicine. 2020; 45: (4).

Yue J, Chen L, Cabrera AR, et al. Measuring tumor cell proliferation with 18F-FLT PET during radiotherapy of esophageal squamous cell carcinoma: A pilot clinical study. Journal of Nuclear Medicine. 2010; 51(4):528–534.

Yun M, Oh SJ., Ha HJ, Ryu JS, Moon DH. High radiochemical yield synthesis of 3'-deoxy-3'-[18F]fluorothymidine using (5'-O-dimethoxytrityl-2'-deoxy-3'-O-nosyl-β-D-threo pentofuranosyl) thymine and its 3-N-BOC-protected analogue as a labeling precursor. Nuclear Medicine and Biology. 2003; 30(2):151-157.

Zade A, Purandare N, Rangarajan V, et al. Noninvasive approaches to diagnose intrathoracic extramedullary hematopoiesis 18F-FLT PET/CT and 99mTc-SC SPECT/CT scintigraphy. Clin Nucl Med. 2012; 37:788-789.

Zanoni L, Broccoli A, Lambertini A, et al. Role of 18F-FLT PET/CT in Suspected Recurrent or Residual Lymphoma: Final Results of a Pilot Prospective Trial. European Journal of Nuclear Medicine and Molecular Imaging. 2019; 46:1661–1671.

Zhao F, Li M, Wang Z, et al. 18F-Fluorothymidine PET-CT for resected malignant gliomas before radiotherapy: tumor extent according to proliferative activity compared with MRI. PLOS ONE. March 4, 2015.

Zhao F, Cui Y, Li M, et al. Prognostic value of 3'-Deoxy-3'-18F-Fluorothymidine ([18F] FLT PET) in patients with recurrent malignant gliomas. Nuclear Medicine and Biology. 2014; 41: 710–715.

Zander T, Scheffler M, Nogova L, et al. Early prediction of nonprogression in advanced non–small-cell lung cancer treated with erlotinib by using [18F]fluorodeoxyglucose and [18F]fluorothymidine positron emission tomography. J Clin Oncol, 2011.

Zhang G, Han D, Ma C, et al. Gradient-based delineation of the primary GTV on FLT PET in squamous cell cancer of the thoracic esophagus and impact on radiotherapy planning. Radiation Oncology. 2015: 10:11.